International
Progress Report

IPR-01-58

Äspö Hard Rock Laboratory

Single-hole hydraulic tests and short-term interference tests in KI0025F03

Bengt Gentzschein
Jan-Erik Ludvigson

GEOSIGMA AB

January 1999

Svensk Kärnbränslehantering AB
Swedish Nuclear Fuel
and Waste Management Co
Box 5864
SE-102 40 Stockholm Sweden
Tel +46 8 459 84 00
Fax +46 8 661 57 19

Äspö Hard Rock
Laboratory

Report no.	No.
IPR-01-58	F56K
Author	Date
Gentzschein, Ludvigson	00-01-01
Checked by	Date
Anders Winberg	00-04-04
Approved	Date
Christer Svemar	02-08-23

Äspö Hard Rock Laboratory

Single-hole hydraulic tests and short-term interference tests in KI0025F03

Bengt Gentzschein
Jan-Erik Ludvigson

GEOSIGMA AB

January 1999

Keywords: TRUE, single-hole hydraulic tests, interference tests

Abstract

The characterisation work for the TRUE Block Scale Project started at Äspö during 1996. Characterisation data from a number of boreholes have been used to update the structural model of the TRUE Block Scale rock volume. Based on the structural model and the identified need for a new borehole to be used for tracer tests, the borehole KI0025F03 was completed.

This report describes the flow and pressure build-up tests conducted in intervals of KI0025F03. In total, 13 tests were performed with a packer spacing of 2 m. The objectives of the tests were to estimate hydraulic parameters and, if possible, to identify flow models. The tests were performed as constant-rate withdrawal tests with duration of c. 30 minutes, followed by a pressure build-up period of c. 45 minutes. The tests aimed at lowering the ambient pressure in the test interval with c. 2 Mpa (200 m). The underground hydraulic test system (UHT 1) developed by SKB was used.

During the flow- and pressure build-up tests, the pressure interference was also registered in sections of the surrounding boreholes, connected to the HMS-system. Comprehensive responses in several boreholes occurred during four of the tests. During the other tests only a few observation sections, or no sections at all, responded, probably due to the low hydraulic conductivity and flow rate of the sink sections.

Firstly, the pressure responses were evaluated quantitatively and plotted in diagnostic response diagrams and time-distance-drawdown diagrams. The responses during all tests were summarised in a pressure response matrix. On the basis of this matrix, the results were compared with the current structural model and checked for consistency. Secondly, a quantitative (time-drawdown) analysis was made on the most significant pressure responses during the tests with comprehensive responses. This analysis also involved a deduction of the dominating flow geometry during the tests.

The qualitative evaluation indicated that the results of the interference tests in general were consistent with the structural model. The quantitative evaluation gave consistent results regarding transmissivity and storativity for the tests analysed and also with previous tests in the TRUE Block Scale rock volume. The dominating flow regime during the tests was (pseudo)-radial flow, in some cases transiting to leaky (pseudo-spherical) flow by the end of the tests.

Sammanfattning

Karakteriseringsarbetet för TRUE Block Scale Project vid Äspö HRL startade under 1996. Karakteriseringsdata från ett antal borrhål har använts för att uppdatera strukturmodellen av TRUE Block Scale volymen. Borrhål KI0025F03 fullbordades baserat på strukturmodellen och det identifierade behovet att använda ett nytt borrhål i spårämnesförsöken,.

Denna rapport beskriver flödes- och tryckuppbyggnadstester i sektioner av borrhål KI0025F03. Totalt utfördes 13 tester med ett manschettavstånd på 2 m. Syftet med testerna var att bestämma hydrauliska parametrar och, om möjligt, att identifiera flödesmodeller. Testerna utfördes som pumptester med konstant flöde med ca. 30 minuters varaktighet, följt av en tryckuppbyggnadsperiod av ca. 45 minuter. I testerna sänktes det omgivande trycket i testintervallerna med ca. 2 MPa (200 m). Testsystemet UHT 1, utvecklat av SKB, användes vid testerna.

Under flödes- och tryckuppbyggnadstesterna registrerades också tryckresponser i sektioner av omgivande borrhål, anslutna till HMS-systemet. Stora responser uppmättes i flera borrhål under fyra av testerna. Under de andra försöken svarade endast några borrhålssektioner eller inga sektioner alls, troligen p g a låg hydraulisk konduktivitet och flöde i de sektioner som fungerade som sänkor.

Först utvärderades tryckresponserna kvantitativt och plottades i diagnostiska responsdiagram och tid-distans-avsänkningsdiagram. Responserna från alla försök summerades i en tryckresponsmatris. Baserat på denna matris jämfördes resultaten med nuvarande strukturmodell och överensstämmelsen kontrollerades. Sedan gjordes en kvantitativ (tid-avsänkning) analys på de mest signifikanta tryckresponserna under testerna med stora responser. Denna analys involverar även en utvärdering av den dominerande flödesgeometrin under försöken.

Den kvalitativa utvärderingen indikerade att resultatet av interferenstesterna generellt överensstämmer med strukturmodellen. Den kvantitativa utvärderingen gav överensstämmande resultat gällande transmissivitet och magasinskoefficient för de analyserade testerna och även med föregående tester i TRUE Block Scale volymen. Den dominerande flödesregimen under testerna var (pseudo)-radiellt flöde, i några fall övergående till läckande (pseudo-sfäriska) flöden i slutet av testerna.

Contents

List of Figures

List of Tables

1 Introduction and objectives

During 1996 characterisation work for the TRUE Block Scale Project commenced at Äspö with drilling of borehole KA2563A from the spiral tunnel. Characterisation data from this borehole and data from boreholes KA2511A, KA3510A, KI0025F, KI0023B and KI0025F02 have been used to update the reconciled structural model (March 1999) of the south-western part of the True Block Scale rock volume (Hermanson, in prep., Doe 1999). Based on the March 99 model and the identified need for a new borehole to be used for the planned tracer tests, an additional borehole, KI0025F03, has been completed.

Borehole KI0025F03 has been characterised with borehole TV (RAAX-BIPS), and POSIVA Flow logging. The results have served as an input to the selection of the test intervals of the flow and pressure build-up tests in KI0025F03.

This report documents the methods and results of the "Selective Flow and Pressure Build-up Tests" performed in Borehole KI0025F03 from October 4 – October 11, 1999.

The general objective of the selective flow and pressure build-up tests was to provide detailed information regarding the hydraulic characteristics of features in borehole KI0025F03 which may be regarded as boundaries to, or potential target features of, future block scale transport experiments. Cross-hole responses during the flow and pressure build-up tests are of particular interest to assess connectivity and thus provide preliminary data for optimising the configuration of the multi-packer system to be installed in KI0025F03. Furthermore, the results will be compared with the structural (March 99) model and checked for consistency with this model.

2 Scope of testing

Borehole KI0025F03 is drilled S-SW (bearing 207º) with a downward inclination of 29.8º to a total length of 141.7 m. The nominal diameter of the hole is 76 mm. The preliminary core mapping, the driller's log and the available BIPS images show that the borehole samples an essentially homogeneous body of Äspö diorite. Occasional minor bodies of greenstone and fine-grained granite are intersected at some locations.

The tests were performed in selected test sections of borehole KI0025F03, using double packer arrangement. The packer spacing was two metres. Tentative target intervals for the tests were selected based on observed inflow during drilling and on the updated and reconciled structural model of the TRUE Block Scale Volume (Hermansson in prep., Doe 1999). The final selection was based on results from borehole TV (BIPS) and POSIVA flow logging. The tested intervals (sections) in KI0025F03 are summarised in Table 2-1 together with the associated structures and measured inflows from the POSIVA flow logging (Rouhiainen and Heikkinen 1999).

Table 2-1. Constant flow tests and pressure build-up tests conducted in KI0025F03, October 1999.

Test No	Section (m)	Date of test	Structure #	Inflow (l/min)	Geology
1	42.5 – 44.5	991005	7	1.5	Main fault at 43.0 m and 2 single parallel 43.2 m and 43.4 m
2a	52.0 – 54.0	991005	?	0.6	One single parallel at 53.65 m.
2b	51.5 – 53.5	991006	6	5.0	Main fault at 51.95 m
3	54.0 – 56.0	991006	?	0.2	Two single parallel to main fault at 55.2 and 55.5 m.
4	56.0 – 58.0	991006	?	0.04	Single parallel to main fault at 57.2 m.
5	60.0 – 62.0	991006	22	0.8	Main fault at 61.2 m and single fracture at 60.7 m.
6	62.0 – 64.0	991007	?	0.05	Single fracture at 63.2 m
7	72.0 – 74.0	991007	20	1.8	Minor fracture zone 7-8 cm wide at 73.1 m.
8	85.0 – 87.0	991007	?	0.1	Single fracture in "good rock"
9	87.0 – 89.0	991008	21	1.5	Main fault at 87.4 m and single parallel fractures at 87.25, 87.35 and 87.75 m.
10	90.5 – 92.5	991008	13	0.5	Main fault at 91.9 m and single fractures at 91.1 and 91.4 m.
11	98.0 – 100.0	991011	?	0.2	3-4 minor fractures with varying orientations.
12	124.0 – 126.0	991011	19	2.0	Main fault at 124.6 m and single parallel at 125.5 m.

3 Performance

3.1 Equipment used

The underground hydraulic test system (UHT 1) developed by SKB (Almén and Hansson, 1996) was used for the tests in KI0025F03. The UHT is documented in detail in Adams (1998) and Gentzschein and Morosini (1998). UHT 1 is constructed for underground hydraulic testing in 56 mm and 76 mm diameter boreholes. Maximum borehole length is 300 m and the maximum working depth is 500 metres below sea level. The main parts of the system are:

- **Down-hole System**: including packer system (double or single) for isolating the target test interval, down-hole shut-in valve, central tubing, and control lines for packer inflation and pressure measurement.
- **Hoisting Rig**: for installing and removing the packer system.
- **Surface System**: including data acquisition, flow meters, flow and pressure control and measurement equipment.

The down-hole system includes a flow bypass that connects the guard intervals below the lower packer and above the upper packer (i.e. the entire borehole except the test interval).

There are two sets of transducers with different pressure ranges. The standard set of pressure transducers is:

Interval/packer	Number	Transducer id	Range	(alternative range)
Test section	2	P and P_b	6 MPa	(1 MPa)
Borehole	1	P_a	6 MPa	(1 MPa)
Packers	1	P_{pack}	8 MPa	(2 MPa)

The flow meter unit enables monitoring and regulation of the flow during constant pressure tests and constant rate tests, respectively. The flow regulation is operated and controlled using a digital computer. There are two mass flow meters, Q_{small} and Q_{big}, of type Coriolis-meters. The flow range is 0.001-100 L/min.

During the tests designated as “Cross-Hole Tests”, the HMS Data Acquisition System was used for collection of data in the observation intervals.

3.2 Single-hole tests

The tests were performed as constant-rate withdrawal tests (CFW), followed by a pressure build up period (CPBU). The constant flow tests aimed at lowering the ambient pressure in the test section with c.2 MPa (200 m water column). Half the total flow rate measured by the POSIVA flow logging within the actual test intervals was chosen for the tests. The resulting pressure was registered as a function of time. Subsequently the test section was shut in and the pressure was allowed to recover to ambient pressure.

3.2.1 Test Cycle and Procedures

The test cycle adopted for the flow and pressure build up tests in borehole KI0025F03, after mobilisation on the borehole, was the following;

1 . The packer assembly was inserted to the desired test location using the hoisting rig. Estimated duration: 5 - 30 minutes depending on the distance to the (next) test position.

2. Packer expansion waiting for creeping effects in the packer material (polyurethane) to diminish enough to permit start of test.
   Time: Minimum 20 minutes.

3. Evacuation of air from the pipe string and the measurement hose.

4 . Opening of test valve and regulation of water flow under constant rate conditions (Flow Phase) during which the flow and the test interval pressure was registered as a function of time. The exact length of the flow phase was decided on the basis of plots of flow as a function of time generated by the system.
   Time: 30 minutes.

5. Closing of test valve followed by pressure recovery (Build-up Phase) during Which pressure was registered as a function of time.
   Time: 45 minutes.

6. Packer deflation. Time: 3 - 5 minutes.

7. Transfer of packer assembly to the next test section.
   Estimated time: 5 - 30 minutes depending on the distance to the next test position.

3.2.2 Calibration

The flow meters Q_{small} and Q_{big}, see chapter 3.1, were calibrated using graduated cylinders and the clock of the measurement computer. Two flows were measured for each flow meter for the purpose of calibration, and each level was measured twice.

The pressure transducers P_a , P_b and P_{pack}, see chapter 3.1, were calibrated with the help of the reference pressure system established in the Äspö HRL tunnel. The transducers were connected to two hoses, filled with water of known density. The hoses respectively lead up to two different but known reference water levels (at KK0120 and KK2850) along the tunnel. The datums are well determined which enables calculation of the calibration constants. The position of the pressure sensors and the barometric pressure are also used in the calibration process. The elevation of the sensors were surveyed prior to the tests and the barometric pressure was measured with a Druck DPI 700 digital pressure indicator, which have a factory-listed accuracy of 0.05% of full scale (2 bar).
The temperature sensor and the electric conductivity sensor were only zero-point calibrated. The temperature sensor was compared with a high-accuracy portable thermometer of good quality. The conductivity sensor was calibrated using a liquid solution with a well-defined electric conductivity.
The results of the calibrations were inputted into the measurement computer and the calibration constants were automatically calculated.

3.2.3 Data Processing

The parameters, measured by the UHT-1 measurement system are:

P	Pressure of the test interval
P_a	Pressure of the borehole intervals around the test interval
P_{pack}	Packer pressure
T_{surf}	Water temperature (surface)
Q_1	Water flow rate Q_{small}
Q_2	Water flow rate Q_{big}
P_b	Pressure of the test interval (same as P)
Elcond	Electrical conductivity

Input data are processed by various programs of the measurement computer, see Gentzschein and Morosini 1998. Three types of diagrams are produced (c.f. Appendix 1):

- A diagrams (**A1 - A5**) show pressure, flow and temperature variations during the whole test cycle. **A0** is a flyleaf showing background data as well as measured and calculated data from the test.
- B diagrams (**B1 - B6**) show pressure and flow variations during the flow phase in logarithmic and semilogarithmic scale. Also other parameter transformations are plotted.
- C diagrams (**C1 - C9**) show pressure and flow variations during the pressure build-up phase in logarithmic and semi-logarithmic scale. Also other transformations of parameters and time are plotted.

Appendix 1 describes the symbols and the parameters of the diagrams.

3.2.4 Performance

In the following, the performance of each test is described together with test controlling parameters and test data are compiled.

Section 42.5 - 44.5 m

A first attempt, starting at 15.41 was interrupted, since the pre-set flow rate was too low. The test was restarted 16.40. The packer pressure was not released between the two tests. The flow rate is somewhat unstable during the outflow period. Test controlling parameters and test data are compiled in the table below.

Parameter	Unit	Value	Explanation
Po	(kPa)	4273.94	Initial formation pressure
P	(kPa)	variable	Section pressure
dPom	(kPa)	3649.91	Average of Po - P during flow phase
tp	(s)	2330	Flowing time
Qp	(m^3/s)	$1.067 \cdot 10^{-5}$	Flow rate at the end of flow phase
dtf	(s)	3009	Recovery time
Koss	(m/s)	$9.75 \cdot 10^{-9}$	Steady state hydraulic conductivity

Section 52.0 - 54.0 m

The pre-set flow-rate value was $4.17 \cdot 10^{-5}$ m^3/s (2.5 l/min). However, the interval was less permeable than expected. The flow decreases from 2.1 l/min to c. 0.87 l/min, while the section pressure is low at a constant level. Test controlling parameters and test data are compiled in the table below.

Parameter	Unit	Value	Explanation
Po	(kPa)	4263.5	Initial formation pressure
P	(kPa)	variable	Section pressure
dPom	(kPa)	3871.53	Average of Po - P during flow phase
tp	(s)	2041	Flowing time
Qp	(m^3/s)	$1.48 \cdot 10^{-5}$	Flow rate at the end of flow phase
dtf	(s)	23716	Recovery time
Koss	(m/s)	$1.27 \cdot 10^{-8}$	Steady state hydraulic conductivity

Section 51.5 - 53.5 m

This test interval was chosen to cover the main fault intersecting the borehole at 51.95 m borehole length. When planning the tests the fault was assumed to intersect the borehole at 52.0 m. As in the previous test the pre-set flow rate ($4.17 \cdot 10^{-5}$ m^3/s, 2.5 l/min) cannot be maintained. Test controlling parameters and test data are compiled in the table below.

Parameter	Unit	Value	Explanation
Po	(kPa)	4306.71	Initial formation pressure
P	(kPa)	variable	Section pressure
dPom	(kPa)	3894.47	Average of Po - P during flow phase
tp	(s)	2089	Flowing time
Qp	(m^3/s)	$3.797 \cdot 10^{-5}$	Flow rate at the end of flow phase
dtf	(s)	3156	Recovery time
Koss	(m/s)	$3.25 \cdot 10^{-8}$	Steady state hydraulic conductivity

Section 54.0 - 56.0 m

About nine and nineteen minutes respectively from the flow start, the stable flow was interrupted by a disturbance of unknown origin. Test controlling parameters and test data are compiled in the table below.

Parameter	Unit	Value	Explanation
Po	(kPa)	4236.02	Initial formation pressure
P	(kPa)	variable	Section pressure
dPom	(kPa)	591.74	Average of Po - P during flow phase
tp	(s)	1929	Flowing time
Qp	(m^3/s)	$1.563 \cdot 10^{-6}$	Flow rate at the end of flow phase
dtf	(s)	2724	Recovery time
Koss	(m/s)	$8.81 \cdot 10^{-9}$	Steady state hydraulic conductivity

Section 56.0 - 58.0 m

The pre-set flow rate was 0.02 l/min ($3.33 \cdot 10^{-7}$ m^3/s). However, the regulation system was not able to establish a steady flow at this level. The target value was increased to 0.03 l/min, which stabilised the flow rate. Later during the flow phase the measurement computer stopped working for some 16 minutes. During the monitoring interruption the regulation valves were working and the flow was kept at the pre-set level. Test controlling parameters and test data are compiled in the table below.

Parameter	Unit	Value	Explanation
Po	(kPa)	4230.80	Initial formation pressure
P	(kPa)	variable	Section pressure
dPom	(kPa)	594.81	Average of Po - P during flow phase
tp	(s)	3896	Flowing time
Qp	(m^3/s)	$4.944 \cdot 10^{-7}$	Flow rate at the end of flow phase
dtf	(s)	2936	Recovery time
Koss	(m/s)	$2.77 \cdot 10^{-9}$	Steady state hydraulic conductivity

Section 60.0 - 62.0 m

A stable flow is achieved after 3-4 minutes. The borehole pressure outside the test interval increased during flow period as well as the during the recovery period. Test controlling parameters and test data are compiled in the table below.

Parameter	Unit	Value	Explanation
Po	(kPa)	4423.21	Initial formation pressure
P	(kPa)	variable	Section pressure
DPom	(kPa)	1470.17	Average of Po - P during flow phase
tp	(s)	1857	Flowing time
Qp	(m^3/s)	$6.666 \cdot 10^{-6}$	Flow rate at the end of flow phase
dtf	(s)	3724	Recovery time
Koss	(m/s)	$1.51 \cdot 10^{-8}$	Steady state hydraulic conductivity

---

Section 62.0 - 64.0 m

As was the case with the previous test, the borehole pressure increased throughout the flow period and during the recovery. Test controlling parameters and test data are compiled in the table below.

Parameter	Unit	Value	Explanation
Po	(kPa)	4418.24	Initial formation pressure
P	(kPa)	variable	Section pressure
dPom	(kPa)	3804.85	Average of Po - P during flow phase
tp	(s)	1837	Flowing time
Qp	(m^3/s)	$5.200 \cdot 10^{-7}$	Flow rate at the end of flow phase
dtf	(s)	2719	Recovery time
Koss	(m/s)	$4.56 \cdot 10^{-10}$	Steady state hydraulic conductivity

---

Section 72.0 - 74.0 m

A first attempt, starting at 15.34 was interrupted due to a mismanoeuvre at the flow start. The test valve was open for just some seconds. The test was restarted 16.11. The packer pressure was not released between the two tests. Test controlling parameters and test data are compiled in the table below.

Parameter	Unit	Value	Explanation
Po	(kPa)	4466.30	Initial formation pressure
P	(kPa)	variable	Section pressure
dPom	(kPa)	464.83	Average of Po - P during flow phase
tp	(s)	1903	Flowing time
Qp	(m^3/s)	$1.490 \cdot 10^{-5}$	Flow rate at the end of flow phase
dtf	(s)	2724	Recovery time
Koss	(m/s)	$1.07 \cdot 10^{-7}$	Steady state hydraulic conductivity

---

Section 85.0 - 87.0 m

After flow stop the pressure recovered over the night. Test controlling parameters and test data are compiled in the table below.

Parameter	Unit	Value	Explanation
Po	(kPa)	4456.49	Initial formation pressure
P	(kPa)	variable	Section pressure
dPom	(kPa)	2136.68	Average of Po - P during flow phase
tp	(s)	1807	Flowing time
Qp	(m^3/s)	$8.333 \cdot 10^{-7}$	Flow rate at the end of flow phase
dtf	(s)	45127	Recovery Flowing time
Koss	(m/s)	$1.30 \cdot 10^{-9}$	Steady state hydraulic conductivity

---

Section 87.0 - 89.0 m

A first attempt, starting at 07.46 was interrupted since a stable flow was not achieved. The test valve was open between 08:12.30 and 08:16. The test was restarted 08.22 with a valve opening at c. 08:45. The packer pressure was not released between the two tests. Test controlling parameters and test data are compiled in the table below.

Parameter	Unit	Value	Explanation
Po	(kPa)	4492.85	Initial formation pressure
P	(kPa)	variable	Section pressure
dPom	(kPa)	1952.85	Average of Po - P during flow phase
tp	(s)	1851	Flowing time
Qp	(m^3/s)	$1.319 \cdot 10^{-5}$	Flow rate at the end of flow phase
dtf	(s)	3024	Recovery time
Koss	(m/s)	$2.25 \cdot 10^{-8}$	Steady state hydraulic conductivity

---

Section 90.5 - 92.5 m

The flow rate and the pressure are stable during the end of the flow period. The data curve from the recovery period is also rather flat. Test controlling parameters and test data are compiled in the table below.

Parameter	Unit	Value	Explanation
Po	(kPa)	4614.06	Initial formation pressure
P	(kPa)	variable	Section pressure
dPom	(kPa)	2969.84	Average of Po - P during flow phase
tp	(s)	1816	Flowing time
Qp	(m^3/s)	$1.319 \cdot 10^{-5}$	Flow rate at the end of flow phase
dtf	(s)	3259	Recovery time
Koss	(m/s)	$5.58 \cdot 10^{-9}$	Steady state hydraulic conductivity

---

Section 98.0 - 100.0 m

The pressure trend during the packer inflation period and during the recovery indicates that the formation pressure was recovering during the test. A possible explanation is that the time to transfer the double packer to the test position was longer than normal. Test controlling parameters and test data are compiled in the table below.

Parameter	Unit	Value	Explanation
Po	(kPa)	4448.63	Initial formation pressure
P	(kPa)	variable	Section pressure
dPom	(kPa)	897.26	Average of Po - P during flow phase
tp	(s)	2007	Flowing time
Qp	m^3/s)	$1.666 \cdot 10^{-6}$	Flow rate at the end of flow phase
dtf	(s)	2977	Recovery time
Koss	(m/s)	$6.19 \cdot 10^{-9}$	Steady state hydraulic conductivity

---

Section 124..0 – 126.0 m

Test controlling parameters and test data are compiled in the table below.

Parameter	Unit	Value	Explanation
Po	(kPa)	4788.56	Initial formation pressure
P	(kPa)	variable	Section pressure
dPom	(kPa)	1391.90	Average of Po - P during flow phase
tp	(s)	1929	Flowing time
Qp	m^3/s)	$1.679 \cdot 10^{-5}$	Flow rate at the end of flow phase
dtf	(s)	5452	Recovery time
Koss	(m/s)	$4.02 \cdot 10^{-8}$	Steady state hydraulic conductivity

---

3.3 Interference tests

3.3.1 Pressure monitoring in the observation boreholes

The pressure histories in all boreholes connected to the HMS-system were monitored during the interference test periods. During these periods the HMS-system was set to only store a pressure value if the change of pressure was more than 1 kPa compared to the previous value. The scanning density for pressure was set to 2 seconds throughout the tests. Observation borehole sections with a total drawdown ≥ 1 kPa at stop of flowing were identified for all tests and report files (MIO-files) were prepared for these boreholes.

3.3.2 Data processing

From the MIO-files, drawdown and recovery files were generated using the SKB software PUMPKONV together with the corresponding drawdown and recovery derivatives. Drawdown (and –derivative) was generated as a function of time and the recovery (and –derivative) as a function of equivalent time (dte). The corresponding plots were generated by the SKB software SKBPLOT.

4 Evaluation

4.1 Single-hole tests

The test interpretation will be conducted using standard analytical models to produce hydraulic coefficients for the test intervals. The interpretation is intended to provide basic results relatively soon after testing is completed.

Objectives of the interpretation are the following:

- Flow geometry and Flow-model identification (if possible)
- Estimates of hydraulic parameters (T and K_e)
- Structure identification through interference test responses

The flow geometry and flow-model identification will be conducted using the diagnostic plots discussed above. Once the various parts of the well response have been identified (i.e. inner boundary, basic flow model and outer boundary), the appropriate analytical method will be applied.

4.1.1 Constant-rate Tests

For constant rate tests, a straight-line is fit to the indicated data set on a semi-log graph of Δp (or Δh) vs. log time. Transmissivity was estimated using the following equation (Cooper & Jacob, 1946):

$$T = \frac{2.3Q}{4\pi m}$$

where:

Q =	flow rate	[m3/s]
m =	slope of straight line	[m/log cycle]

Experience at the Äspö HRL is that the flow responses normally observed suggest a flow dimension of nearly 3 (spherical flow). Therefore, responses indicating near steady state are analysed using a steady-state approximation formula developed by Moye, (1967) for spherical flow. The formula can be applied to both constant pressure and constant rate data.

$$T = \left[\frac{Q_p}{\Delta h}\right]\left[\frac{1+\ln\left(L/2r_w\right)}{2\pi}\right]$$

where:

T =	transmissivity [m2/s]
Q_p=	flow at the end of the flow phase[m3/s]
Δh =	pressure drop in the test section expressed in meters of water[m]
L =	interval length [m]
r_w =	borehole radius[m]

In addition, the specific capacity (Q/Δh) was calculated for each flow test based on the flow rate and drawdown at the end of the flow period. This is calculated as a standard comparative value for tests conducted at the Äspö HRL.

4.1.2 Pressure Build-up Tests

The pressure build-up period can be analysed in a comparable manner to a constant rate test. If steady-state conditions were established prior to shut-in, the analysis is identical to that of the flow test. If no steady-state conditions were reached (i.e. infinite-acting radial flow at the end of the period), then the effects of the proceeding flow period must be accounted for. Because steady-state conditions are generally reached in the flow tests at the HRL, it is normally not necessary to account for the previous flow period.

For cases in which steady-state conditions are not reached, diagnostic plots are prepared according to Agarwal (1980), who presented a relationship that plots the recovery pressure change versus an equivalent time instead of elapsed time. The equivalent time function essentially converts the pressure recovery event to an equivalent constant rate test response that can be analysed using the straight-line analysis method presented above. Equivalent time is calculated using the following formula:

$$dt_e = \frac{t_p \cdot dt}{t_p + dt}$$

where:

dte =	equivalent time	[s]
tp =	duration of preceding flow period	[s]
dt =	elapsed recovery time	[s]

4.2 Interference tests

4.2.1 Qualitative evaluation

The hydraulic responses are evaluated in different steps in which part of the data has been sorted out for further (quantitative) evaluation. The qualitative evaluation involves preparation of pressure response diagrams for each test and a common pressure response matrix for all tests. In addition, drawdown versus time-distance diagrams (s versus t/R^2), similar to the pressure response diagrams, and pressure derivative curves are also used in the qualitative evaluation. The latter two methods are described in the quantitative evaluation below.

Time-drawdown (and recovery) plots were prepared for sections showing a total drawdown of more than s_p=0.1 m (1 kPa) at stop of the flow period. This minimal drawdown value is the same as the threshold value used for the pressure registration in the observation boreholes, see Section 3.3. From these plots, the response times (t_R) for each section were estimated. The response time is here defined as the time after start of flowing when a drawdown (or recovery) of 1 kPa is observed (from the logarithmic plots) in the actual observation section. The qualitative evaluation has mainly been made on data from the drawdown phase. Data from the recovery phase were used as supporting data. For example, during some of the tests there were uncertainties in the drawdown data due to trends in the background pressure during testing.

On the X-axis of the pressure response diagrams, the ratio of the response time (t_R) and the (squared) straight-line distance R between the (midpoint of) the source section and (the midpoint of) each observation section (t_R/R^2) is plotted. The latter ratio is inversely related to the hydraulic diffusivity of the rock, which indicates the speed of propagation in the rock of the drawdown created in the flowing section.

The final drawdown at stop of flowing (s_p) in the responding sections were determined from the drawdown files. To account for the different flow rates used in the tests and to make the pressure response plots comparable between tests, the final drawdown is normalised with respect to the flow rate (Q). The ratio s_p/Q is plotted on the Y-axis of the pressure response diagrams.

From the response plots of s_p/Q versus t_R/R^2 for each test, sections with anomalous, fast response times (high hydraulic diffusivity) and large (normalised) drawdown can be identified. Such sections, showing primary responses, can be assumed to have a distinct hydraulic connection to the flowing section and may be intersected by a single fracture; fracture zones or other conductive structures in the rock. On the other hand, sections with delayed and weak (secondary) responses may correspond to sections in the rock mass between such structures.

From the calculated values of s_p/Q (index 1) and t_R/R^2 (index 2) for each observation section during each test, a common pressure response matrix showing the response patterns for all tests, was prepared by classifying the pressure responses by means of the above indexes 1 and 2. For index 1, the following class limits and drawdown characteristics were used:

Index 1 (s_p/Q)

$s_p/Q > 1 \cdot 10^5$ s/m^2	Excellent
$3 \cdot 10^4 < s_p/Q \leq 1 \cdot 10^5$ s /m^2	High
$1 \cdot 10^4 < s_p/Q \leq 3 \cdot 10^4$ s /m^2	Medium
$s_p/Q \leq 1 \cdot 10^4$ s /m^2	Low

For index 2 the following class limits and response characteristics were used:

Index 2 (t_R/R^2)

$t_R/R^2 < 0.01$ s/m^2	Excellent (E)
$0.01 \leq t_R/R^2 < 0.1$ s/m^2	Good (G)
$0.1 \leq t_R/R^2 < 0.3$ s/m^2	Medium (M)
$t_R/R^2 \geq 0.3$ s/m^2	Bad (B)

The results from the qualitative analysis should be compared with the current structural model and the latter checked for consistency and possible need of revision. It should be pointed out that the response diagrams of s_p/Q versus t_R/R^2 described above were only used as diagnostic tools to identify the most significant responses during each test and to construct the response matrix. The diagrams should be used with some care since the true actual distances (along pathways) between the source and observation sections are uncertain which may affect the position of a certain point (i.e. section) in the horizontal direction in the diagrams. However, in most cases, the shortest (straight-line) distance between the source and observation section, as used here, is considered as a sufficient and robust approximation for the above purpose.

Other potential sources of error in the pressure response diagrams may arise from (internal) hydraulic interaction between sections along an observation borehole or active borehole. Such interaction can either be due to packer leakage (insufficient packer sealing) or more likely, due to rock leakage through interconnecting fractures around the packers, possibly both in observation boreholes and in the active borehole. This fact may give a false impression that good hydraulic communication exists between certain observation sections and the actual source section (which is not the fact). However, any analysis method will suffer from this potential source of error.

4.2.2 Quantitative evaluation

The main purpose of the quantitative interpretation of the interference tests in this study is to estimate the hydraulic parameters and the hydraulic characteristics of the most significant responses as identified from the qualitative interpretation. The estimated hydraulic parameters should represent the hydraulic properties of the fracture zones tested. In addition, time-drawdown analysis, including the drawdown derivative, should also provide some (soft) information on the flow geometry during the test and effects of outer hydraulic boundaries. The quantitative evaluation also involved plotting of the most significant responses in a drawdown versus time/distance squared (t/R^2)-diagram.

The derivative of drawdown was used as a diagnostic tool in the interpretation of the flow geometry and deduction of hydraulic boundaries in the time-drawdown analysis. The derivative was generated by the SKB-code PUMPKONV and plotted together with the drawdown versus time curves.

A combination of the Theis' model for pure radial flow in a non-leaky, porous aquifer (Theis 1935) and the Hantush model for a leaky aquifer with no aquitard storage (Hantush and Jacob 1955) was used as interpretation models for the quantitative evaluation. The latter model was used because of its generality and its ability to analyse radial as well as leaky (pseudo-spherical) flow. Tests showing well-defined periods with (pseudo-) radial flow were also analysed by Cooper-Jacob's method (Cooper and Jacob 1946) in semi-logarithmic graphs. The quantitative evaluation was made using the software AquiferTest (Waterloo Hydrologic).

5 Results

5.1 Single-hole tests

5.1.1 Constant Rate- and Pressure Build-up Tests

Relevant test data from the Constant Rate- and Pressure Build-up tests in KI0025F03 are summarised in Table 5-1.

Table 5-1. Test data from the Constant Rate- and Pressure Build-up tests in borehole KI0025F03.

Section (m)	Date of test	Test No	P_o (kPa)	Flowing time (s)	DP (kPa)	DP_a (kPa)	Qp (m^3/sek)	Recovery Time (s)
42.5 – 44.5	991005	1	4273.9	2330	3649.9	27.8	$1.07 \cdot 10^{-5}$	3009
52.0 – 54.0	991005	2a	4263.5	2041	3871.5	52.3	$1.49 \cdot 10^{-5}$	23716
51.5 – 53.5	991006	2b	4306.7	2089	3894.5	40.3	$3.80 \cdot 10^{-5}$	3156
54.0 – 56.0	991006	3	4236	1929	591.7	23.5	$1.56 \cdot 10^{-6}$	2724
56.0 – 58.0	991006	4	4230.8	3896	594.8	24.4	$4.94 \cdot 10^{-7}$	2936
60.0 – 62.0	991006	5	4423.2	1857	1470.2	-9.4	$6.67 \cdot 10^{-6}$	3724
62.0 – 64.0	991007	6	4418.2	1837	3804.9	-9.6	$5.20 \cdot 10^{-7}$	2719
72.0 – 74.0	991007	7	4466.3	1903	464.8	30.9	$1.49 \cdot 10^{-5}$	2724
85.0 – 87.0	991007	8	4456.5	1807	2136.7	8.0	$8.33 \cdot 10^{-7}$	45127
87.0 – 89.0	991008	9	4492.9	1851	1952.9	26.8	$1.32 \cdot 10^{-5}$	3024
90.5 – 92.5	991008	10	4614.1	1816	2969.8	17.8	$4.98 \cdot 10^{-6}$	3259
98.0 – 100.0	991011	11	4448.6	2007	897.3	13.5	$1.67 \cdot 10^{-6}$	2977
124.0 – 126.0	991011	12	4788.6	1929	1391.9	18.4	$1.68 \cdot 10^{-5}$	5452

P_o = Initial formation pressure
DP = Average of the drawdown (Po – P) of the test section during flow phase
DP_a = Drawdown of the borehole interval above and below the test section
Qp = Flow rate at the end of flow phase

The evaluation of the hydraulic parameters is described in Chapter 4. Table 5-2 summarises the results from the single-hole tests in KI0025F03. The transient evaluation of the Pressure Build-up tests in semi-logarithmic diagrams is presented in Appendix 2. During test #1, no transient evaluation could be made due to almost instantaneous steady state during both the Constant flow- and the Pressure Build-up test.

Consistent results were in most cases obtained for the different analysis methods. The dominating flow geometry during the Pressure Build-up tests was a period with (pseudo)-radial flow transiting to leaky (pseudo-spherical) flow and reaching steady state in some tests.

Table 5-2. Summary of Results of Selective Constant Flow- and Pressure Build-up Tests in Borehole KI0025F03.

Test No.	Interval (m)	T_{Moye}	T (CFW) (m^2/s)	T (CPBU) (m^2/s)	Dominating flow geometry	Comment
1	42.5 – 44.5	$2.0 \cdot 10^{-8}$				
					SS	Instantaneous recovery
2a	52.0 – 54.0	$2.6 \cdot 10^{-8}$				Instantaneous drawdown
				$1.4 \cdot 10^{-8}$	Rad→SS	Early-time
2b	51.5 – 53.5	$6.5 \cdot 10^{-8}$	$1.1 \cdot 10^{-7}$			Early-time
				$6.8 \cdot 10^{-8}$	Rad→Leaky	
3	54.0 – 56.0	$1.8 \cdot 10^{-8}$	$1.3 \cdot 10^{-8}$			
				$8.1 \cdot 10^{-9}$	Rad→Leaky	
4	56.0 – 58.0	$5.5 \cdot 10^{-9}$				Unstable flow
				$6.5 \cdot 10^{-9}$	Rad→Leaky	
5	60.0 – 62.0	$3.0 \cdot 10^{-8}$				Instantaneous drawdown
				$8.3 \cdot 10^{-9}$	Rad→Leaky	Early-time
6	62.0 – 64.0	$9.1 \cdot 10^{-10}$	$9.5 \cdot 10^{-10}$			
				$3.3 \cdot 10^{-10}$	Rad→Leaky	
7	72.0 – 74.0	$2.1 \cdot 10^{-7}$	$6.1 \cdot 10^{-7}$			
				$6.1 \cdot 10^{-7}$	Rad	
8	85.0 – 87.0	$2.6 \cdot 10^{-9}$	$1.3 \cdot 10^{-9}$			
				$8.7 \cdot 10^{-10}$	Rad→Leaky	Early-time
9	87.0 – 89.0	$4.5 \cdot 10^{-8}$	$4.4 \cdot 10^{-8}$			
				$3.8 \cdot 10^{-8}$	Rad→Leaky	Early-time
10	90.5 – 92.5	$1.1 \cdot 10^{-8}$	$9.6 \cdot 10^{-9}$			
				$3.9 \cdot 10^{-9}$	Rad→SS	Early-time
11	98.0 – 100.0	$1.2 \cdot 10^{-8}$	$1.7 \cdot 10^{-8}$			
				$6.4 \cdot 10^{-9}$	Rad→Pr. trend	Early-time
12	124 –126	$8.0 \cdot 10^{-8}$				
				$1.3 \cdot 10^{-6}$	Rad→Leaky	

T_{Moye} = Transmissivity according to Moye, see chapter 4.1.1
T (CFW) = Transmissivity from Constant Rate Test, see chapter 4.1.1
T (CPBU) = Transmissivity from Pressure Build-up Test, see chapter 4.1.2
Rad = Radial
Leaky = Pseudospherical (>2D)
SS = Steady-state
Pr. trend = Increasing background pressure trend during the test cycle

5.1.2 Comparison with POSIVA Flow Logging

Prior to the Selective Flow and Pressure Build-up tests, POSIVA Flow Logging was conducted in KI0025F03 as part of the characterisation work (Rouhiainen and Heikkinen 1999). The results of the flow logging are compared to the results of the Constant Flow- and Pressure Build-up Tests. The parameter compared is the specific capacity (C_s). In calculating C_s for the flow logging (**C_s-Posiva)**, it was assumed that the borehole was open and a constant drawdown dH of 400 m was exerted on the flowing intervals. The results are shown in Table 5-3.

Table 5-3. Comparison of Results between POSIVA Flow Logging and Selective Constant Flow- and Pressure Build-up Tests in Borehole KI0025F03.

Selective Flow and Pressure Build-up Tests					POSIVA Flow Logging			
Test No.	**Test Interval**	**dHp** (m)	**Qp** (l/ min)	**C_s -CFW** (m^2/s)	**Flow rate** (l/min)	**dH** (m)	**C_s -Posiva** (m^2/s)	**Ratio C_s -CFW/ C_s-Posiva**
1	42.5 – 44.5	371.88	0.64	$2.9 \cdot 10^{-8}$	1.5	400	$6.3 \cdot 10^{-8}$	0.5
2a	52.0 – 54.0	394.51	0.90	$3.8 \cdot 10^{-8}$	0.6	400	$2.5 \cdot 10^{-8}$	1.5
2b	51.5 – 53.5	396.85	2.28	$9.6 \cdot 10^{-8}$	5	400	$2.1 \cdot 10^{-7}$	0.5
3	54.0 – 56.0	60.30	0.094	$2.6 \cdot 10^{-8}$	0.2	400	$8.3 \cdot 10^{-9}$	3.1
4	56.0 – 58.0	60.61	0.030	$8.2 \cdot 10^{-9}$	0.04	400	$1.7 \cdot 10^{-9}$	4.9
5	60.0 – 62.0	149.81	0.40	$4.5 \cdot 10^{-8}$	0.8	400	$3.3 \cdot 10^{-8}$	1.3
6	62.0 – 64.0	387.71	0.031	$1.3 \cdot 10^{-9}$	0.05	400	$2.1 \cdot 10^{-9}$	0.6
7	72.0 – 74.0	47.37	0.89	$3.2 \cdot 10^{-7}$	1.8	400	$7.5 \cdot 10^{-8}$	4.2
8	85.0 – 87.0	217.73	0.050	$3.8 \cdot 10^{-9}$	0.1	400	$4.2 \cdot 10^{-9}$	0.9
9	87.0 – 89.0	198.99	0.079	$6.6 \cdot 10^{-8}$	1.5	400	$6.3 \cdot 10^{-8}$	1.1
10	90.5 – 92.5	302.63	0.30	$1.6 \cdot 10^{-8}$	0.5	400	$2.1 \cdot 10^{-8}$	0.8
11	98.0 – 100.0	91.43	0.10	$1.8 \cdot 10^{-8}$	0.2	400	$8.3 \cdot 10^{-9}$	2.2
12	124 -126	141.83	1.01	$1.2 \cdot 10^{-7}$	2	400	$8.3 \cdot 10^{-8}$	1.4

C_s –CFW=Qp/dHp=specific capacity from Constant flow tests (Qp and dHp are the flow rate and drawdown, respectively, by the end of the tests).

5.2 Interference tests

5.2.1 Pressure response matrix and response diagrams

The pressure response matrix for interference test #1 to #12 in borehole KI0025F03 is shown in Figure 5-1. The matrix is based on the pressure response diagrams, which show pressure responses ≥1 kPa in the observation borehole sections during the flow (drawdown) phase. The colour and letter coding is based on the two indexes s_p/Q (drawdown normalised to pumping rate) and t_R/R^2 (response time normalised to the square of distance) according to Andersson et al. (1998).

The pressure response diagrams (s_p/Q versus t_R/R^2) during each interference test in KI0025F03 are shown in Appendix 3. The straight-line distances from the sink sections to the receiver sections during the tests are shown in Appendix 5. Distances have only been calculated for responding boreholes.

A potential source of error in interference testing with the UHT-1 system arises from the long, bounding sections at both sides of the tested section. In several of the tests, a small but significant drawdown (dP_a) also occurred in the bounding sections in the tested borehole, c.f. Table 5-1. This drawdown, particularly in the bounding section in front of the test section, most likely also caused secondary (indirect) drawdowns in the outer-most sections in borehole KI0025F02, in particular sections P7, P8 and occasionally in P10. Such clear indirect responses in the latter sections are omitted in the response matrix in Figure 5-1. However, some responses in these sections are still uncertain and may be a combination of direct and indirect responses. In addition, responses in section KI0023B:P3 are also left out due to the problems associated with the instrumentation in this borehole.

Another potential problem for some of the tests is that a certain (increasing) pressure trend occurred during the tests, particularly during tests #5, 6, 8, 10 and #11. This effect is considered negligible in sections with large pressure responses but in sections with small responses this superimposed pressure trend may distort the responses. However, such sections are not of primary interest in this case.

Figure 5-1 shows that comprehensive responses only occurred during tests #2a and #2b and #7 and #9 and to some extent in test #1. During the remainder of the tests only a few sections responded. During tests #3-5, mainly section KI0025F02:P7 responded. However, the (indirect?) responses in this section are uncertain due to reasons discussed above, particularly during tests #1-5 in which the sink sections are located at shallow depths in KI0025F03. Thus, the responses in the outermost sections in KFI0025F02 (P7-P10) may be indirect. Only one observation section responded during tests #4, 10 and 12 whereas no responses at all were obtained during tests #6, 8 and 11, probably due to the low hydraulic conductivity and flow rates of the actual sink sections.

Figure 5-1 indicates that the test responses generally are consistent with the reconciled structural model of March 1999 (Hermansson in prep., Doe 1999). However, test #1 and tests #2a-b indicate that section KI0025F:R5 may be located in structure #7 rather than in #6. This was also indicated by the short-term interference tests in KI0025F02 (Andersson and Ludvigson, 1999).

Tests #2a and 2b support the structural model regarding structure #6. The very strong responses in section KI0025F02:P8, interpreted to be located in structure #6, during these tests are consistent with the structural model. During test #2b, several observation sections respond more rapidly than during test #2a, e.g. section 2563A4, 0023B7 and 0023B6, c.f. Appendix 3. Test #7 clearly supports the structural model regarding structure #20 and also indicates that this structure has good hydraulic connection with #6 (and also with #21). Test #5 supports the structural model regarding structure #22.

The responses during test #9 are generally more delayed and indicate that structure #21 is well connected to structure #6 and 20. The large but delayed responses in sections KI0023B:P4 and KA2563A:S3 are noticeable. Both sections are interpreted to belong to #13 according to the structural model.

5.2.2 Drawdown versus time/(distance)^2-plots

The most significant pressure response sections in the observation boreholes during interference tests #2a, #2b, #7 and #9 in KI0025F03 are shown in drawdown versus time/distance squared (t/R^2)-diagrams in Appendix 4. In a homogenous and isotropic medium all response curves should merge to a common curve.

The figures clearly show that the tested rock is heterogeneous. During tests #2a and #2b section KI0025F02:P8 shows very good responses. The other responses during these tests as well as during test #9 are rather uniform whereas the response pattern during test #7 is more non-uniform. The estimated transmissivity and storativity corresponding to the Theis´-curves shown in the diagrams are shown. The matching (position) of the Theis' curves is rather arbitrarily.

5.2.3 Time-drawdown analysis

Time-drawdown analysis was only made for the most significant responding sections during test #2a, #2b, #7 and #9 in KI0025F02. The results are shown in Tables 5-4 to 5-7. In the tables, the transmissivity, storativity, the hydraulic diffusivity and, if leakance occur, the leakage coefficient (K'/b') are estimated. In addition, the dominating flow geometry during the test and (apparent) hydraulic boundaries are deduced.

The time-drawdown curves (including the drawdown derivative) in the receiver sections indicate a dominating (pseudo)-radial flow geometry during most of the tests. In some of the tests, the radial flow regime was followed by a slight leakance. This is consistent with the results of the single-hole tests, c.f. Section 5.1.1. Due to the short test time, the transition from pseudo-radial flow to leaky flow, as was observed in the sink sections, has not been accentuated in most of the observation sections. In only two of the tests, effects of apparent, outer hydraulic boundaries were noticed.

The calculated values on the hydraulic parameters represent parameters of an equivalent fractured porous medium. Accordingly, the interpretations of flow geometry and hydraulic boundaries also represent such a medium. The estimated values on the hydraulic parameters are fairly consistent between the tests and also with those values presented in Andersson et al. (1999). The values on the leakage coefficient, K'/b', indicate a slight leakance towards the end of the tests.

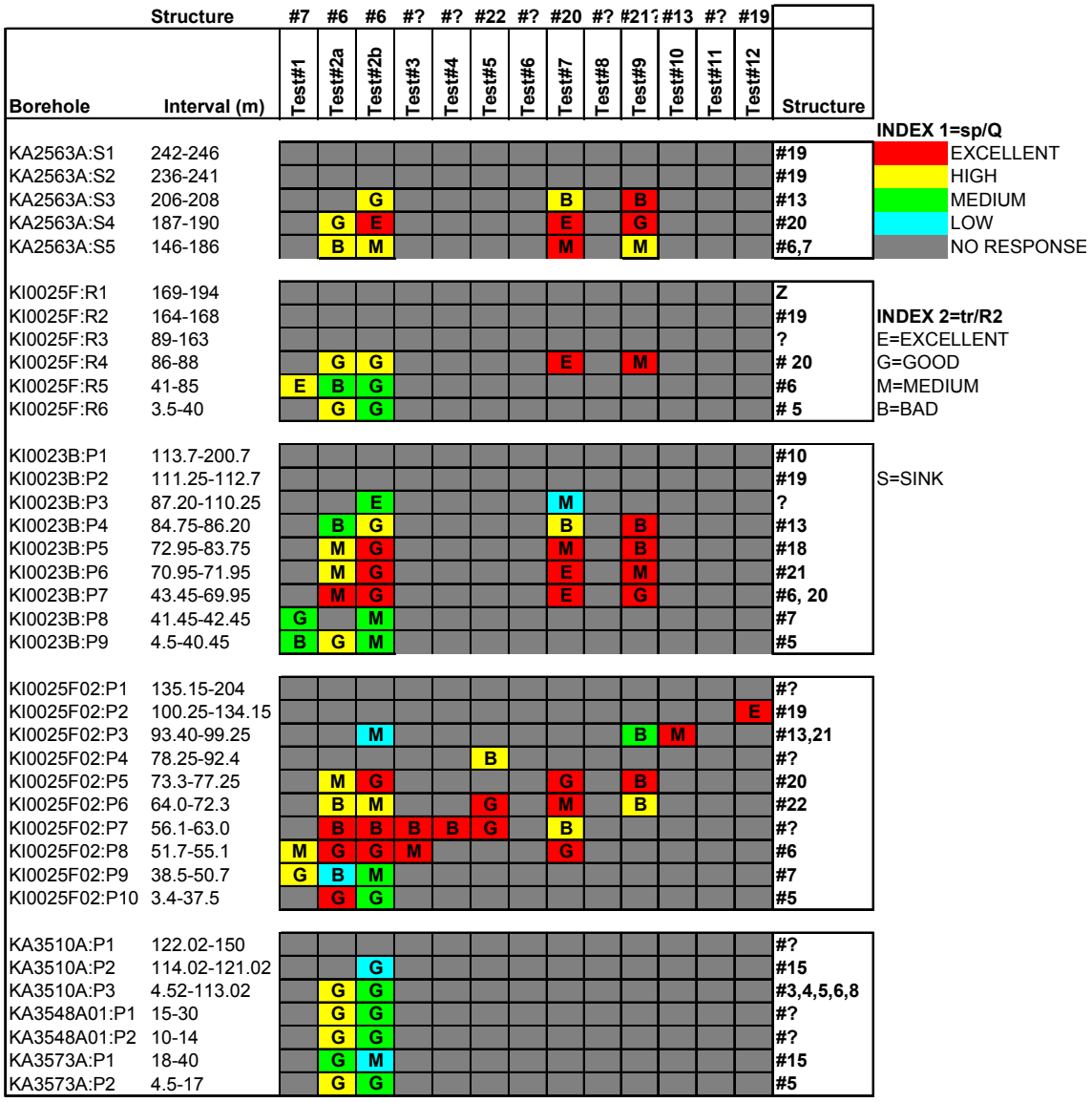

***Figure 5-1**. Pressure response matrix for the interference tests in KI0025F03.*

Table 5-4. Results of time-drawdown analysis of responding sections during the short-term interference test #2a in KI0025F03. T=transmissivity, S=storativity, T/S=hydraulic diffusivity, Rad=Radial, Leaky=pseudospherical (>2D), NFB=Apparent No-flow boundary.

Borehole Section	Structure #	T (m^2/s)	S (-)	T/S (m^2/s)	K'/b' (s^{-1})	Dom. Flow Geometry
KA2563A:S4	20	$2.3 \cdot 10^{-6}$	$7.2 \cdot 10^{-7}$	3.2	$6.6 \cdot 10^{-11}$	Rad→Leaky
KI0025F:R4	20	$3.0 \cdot 10^{-6}$	$5.8 \cdot 10^{-7}$	5.2	-	Rad
KI0025F:R6	5	$3.6 \cdot 10^{-6}$	$9.5 \cdot 10^{-7}$	3.8	-	Rad
KI0023B:P6	21	$2.4 \cdot 10^{-6}$	$1.1 \cdot 10^{-6}$	2.1	-	Rad
KI0023B:P7	6, 20	$2.2 \cdot 10^{-6}$	$1.9 \cdot 10^{-6}$	1.1	-	Rad
KI0023B:P9	5	$3.8 \cdot 10^{-6}$	$4.6 \cdot 10^{-7}$	8.2	-	Rad
KI0025F02:P5	20	$2.5 \cdot 10^{-6}$	$9.5 \cdot 10^{-7}$	2.7	-	Rad
KI0025F02:P7	?	$6.3 \cdot 10^{-7}$	$4.5 \cdot 10^{-6}$	0.14	-	Rad
KI0025F02:P8	6	$1.2 \cdot 10^{-7}$	$9.0 \cdot 10^{-8}$	1.3	$1.7 \cdot 10^{-10}$	Rad→Leaky
KA3510A:P3	3,4,5,6,8	$3.4 \cdot 10^{-6}$	$4.2 \cdot 10^{-7}$	8.0	-	Rad
KA3548A:P1	?	$3.9 \cdot 10^{-6}$	$4.8 \cdot 10^{-7}$	8.1	-	Rad
KA3548A:P2	?	$4.2 \cdot 10^{-6}$	$8.0 \cdot 10^{-7}$	5.3	-	Rad→NFB
KA3573A:P2	5	$4.1 \cdot 10^{-6}$	$2.8 \cdot 10^{-7}$	15	-	Rad

Table 5-5. Results of time-drawdown analysis of responding sections during the short-term interference test #2b in KI0025F03. T=transmissivity, S=storativity, T/S=hydraulic diffusivity, Rad=Radial, Leaky=pseudospherical (>2D), CHB=Apparent Constant-head boundary.

Borehole Section	Structure #	T (m^2/s)	S (-)	T/S (m^2/s)	K'/b' (s^{-1})	Dom. Flow Geometry
KA2563A:S3	13	$1.9 \cdot 10^{-6}$	$2.4 \cdot 10^{-6}$	0.8		Rad
KA2563A:S4	20	$1.8 \cdot 10^{-6}$	$4.3 \cdot 10^{-7}$	3.2	$6.8 \cdot 10^{-11}$	Rad→Leaky
KI0025F:R4	20	$2.2 \cdot 10^{-6}$	$4.0 \cdot 10^{-7}$	5.6	-	Rad
KI0025F:R5	6	$1.5 \cdot 10^{-5}$	$1.5 \cdot 10^{-6}$	10.0	-	Rad
KI0023B:P4	13	$2.3 \cdot 10^{-6}$	$2.3 \cdot 10^{-6}$	1.0	-	Rad
KI0023B:P5	18	$1.8 \cdot 10^{-6}$	$8.1 \cdot 10^{-7}$	2.2	-	Rad
KI0023B:P6	21	$1.9 \cdot 10^{-6}$	$6.5 \cdot 10^{-7}$	2.9	$8.7 \cdot 10^{-11}$	Rad→Leaky
KI0023B:P7	6, 20	$1.5 \cdot 10^{-6}$	$7.8 \cdot 10^{-7}$	2.0	$8.1 \cdot 10^{-11}$	Rad→Leaky
KI0025F02:P5	20	$2.0 \cdot 10^{-6}$	$6.3 \cdot 10^{-7}$	3.2	$4.4 \cdot 10^{-11}$	Rad→Leaky
KI0025F02:P7	?	$6.1 \cdot 10^{-7}$	$5.1 \cdot 10^{-6}$	0.12	-	Rad
KI0025F02:P8	6	$5.6 \cdot 10^{-8}$	$3.4 \cdot 10^{-8}$	1.7	-	Rad→CHB
KA3510A:P3	3,4,5,6,8	$1.4 \cdot 10^{-5}$	$1.4 \cdot 10^{-6}$	10	-	Rad

Table 5-6. Results of time-drawdown analysis of responding sections during the short-term interference test #7 in KI0025F03. T=transmissivity, S=storativity, T/S=hydraulic diffusivity, Rad=Radial, Leaky=pseudospherical (>2D).

Borehole Section	Structure #	T (m^2/s)	S (-)	T/S (m^2/s)	K'/b' (s^{-1})	Dom. Flow Geometry
KA2563A:S4	20	$7.4 \cdot 10^{-7}$	$1.0 \cdot 10^{-7}$	7.5	$8.8 \cdot 10^{-12}$	Rad→Leaky
KI0025F:R4	20	$8.5 \cdot 10^{-7}$	$7.7 \cdot 10^{-8}$	11	-	Rad
KI0023B:P6	21	$8.3 \cdot 10^{-7}$	$2.8 \cdot 10^{-7}$	3.0	$4.0 \cdot 10^{-11}$	Rad→Leaky
KI0023B:P7	6, 20	$8.3 \cdot 10^{-7}$	$1.6 \cdot 10^{-7}$	5.2	$1.7 \cdot 10^{-11}$	Rad→Leaky
KI0025F02:P5	20	$8.3 \cdot 10^{-7}$	$4.3 \cdot 10^{-7}$	1.9	-	Rad
KI0025F02:P6	22	$1.1 \cdot 10^{-6}$	$1.3 \cdot 10^{-6}$	0.82	$1.9 \cdot 10^{-11}$	Rad→Leaky

Table 5-7. Results of time-drawdown analysis of responding sections during the short-term interference test #9 in KI0025F03. T=transmissivity, S=storativity, T/S=hydraulic diffusivity, Rad=Radial, Leaky=pseudospherical (>2D), NFB=Apparent No-flow boundary.

Borehole Section	Structure #	T (m^2/s)	S (-)	T/S (m^2/s)	K'/b' (s^{-1})	Dom. Flow Geometry
KA2563A:S3	13	$3.1 \cdot 10^{-7}$	$4.9 \cdot 10^{-7}$	0.63	-	Rad→NFB
KA2563A:S4	20	$1.1 \cdot 10^{-6}$	$4.2 \cdot 10^{-7}$	2.6	-	Rad
KI0025F:R4	20	$9.4 \cdot 10^{-7}$	$1.1 \cdot 10^{-6}$	0.82	-	Rad→NFB
KI0023B:P4	13	$2.6 \cdot 10^{-7}$	$8.4 \cdot 10^{-7}$	0.30	-	Rad
KI0023B:P6	21	$1.0 \cdot 10^{-6}$	$8.7 \cdot 10^{-7}$	1.2	-	Rad
KI0023B:P7	6, 20	$1.2 \cdot 10^{-6}$	$4.6 \cdot 10^{-7}$	2.5	-	Rad
KI0025F02:P5	20	$8.3 \cdot 10^{-7}$	$4.3 \cdot 10^{-7}$	1.9	-	Rad

6 Conclusions

According to the single-hole tests, interval 51.5-53.5 m (structure #6), 72-74 m (structure #20) and 124-126 m (structure #19) have the highest transmissivity in KI0025F03. The estimated single-hole transmissivity for these intervals ranges from c. $1 \cdot 10^{-7}$ to c. $1 \cdot 10^{-6}$ m^2/s according to different evaluation methods. The dominating flow geometry in the sink sections during the pressure build-up tests was generally a period with pseudo-radial flow transiting to leaky (pseudo-spherical) flow, eventually reaching steady-state flow in some tests.

During the short-term interference tests in KI0025F03, comprehensive responses in the observation sections were only obtained during tests #2a and 2b, #7 and test#9 and to some extent in #1. During the other tests, only one or a few sections responded. During tests #6, 8 and #11 no responses at all were obtained, probably due to the low hydraulic conductivity and flow rates of the actual sink sections.

The results of the interference tests were in general consistent with the reconciled structural model of March 1999. However, test #1 and tests #2a-b indicate that section KI0025F:R5 may be located in structure #7 rather than in #6 which also was indicated from the previous short-term interference tests in KI0025F02. Tests #2a and 2b support the structural model regarding structure #6. During test #2b, several observation sections respond more rapidly than during test #2a, indicating better connectivity with the sink.

Test #7 clearly supports the structural model regarding structure #20 and also indicates that this structure has good hydraulic connection with #6 (and also with #21). The results of test #5 are also consistent with the structural model regarding structure #22 but only a few sections responded during this test.

The responses during test #9 are generally more delayed and indicate that structure #21 may be more diffuse and well connected to structure #6 and 20.

The time-drawdown analysis for tests #2a, 2b, 7 and #9 resulted in consistent estimates of transmissivity and storativity and also consistent with previous tests in the TRUE Block Scale rock volume. The dominating flow regime during these tests was (pseudo)-radial flow, in some cases transiting to slightly leaky (pseudo-spherical) flow towards the end of the tests, which is consistent with the estimated values on the leakage coefficient.

7 References

Adams, J., Andersson P. and Meier, P 1999: TRUE Block Scale Project, Preliminary Results of Selective Pressure Build-up Tests in Borehole KI0025F02. Äspö Hard Rock Laboratory International Progress Report IPR-01-45.

Agarwal, R.G., 1980: A New Method to Account for Producing Time Effects When Drawdown Type Curves Are Used to Analyse Pressure Buildup and Other Test Data. - Soc. of Petroleum Engineers, SPE Paper 9289, presented at SPE-AIME Meeting, Dallas, Texas, September 21-24, 1980.

Almén, K-E and Hansson, K., 1996: Hydrotestutrustning för underjordsmätningar i Äspölaboratoriet – Konstruktion och tillverkning. SKB Internal Report. (In Swedish)

Andersson, P., Ludvigson, J-E., Wass, E., 1998: TRUE Block Scale Project Preliminary Characterisation Stage. Combined interference tests and tracer tests. Performance and preliminary evaluation. Äspö Hard Rock Laboratory International Progress Report IPR-01-44.

Andersson, P., Ludvigson, J-E., Wass, E. and Holmqvist, M., 1999: TRUE Block Scale. Detailed Characterisation Stage. Interference tests and tracer tests PT-1 – PT-4. Äspö Hard Rock Laboratory. International Technical Document IPR-01-52.

Andersson, P. and Ludvigson, J-E., 1999: TRUE Block Scale Project PreliminaryCharacterisation Stage. Tracer dilution tests during pumping in borehole KI0023B and short-time interference tests in KI0025F02 and KA3510A. Äspö Hard Rock Laboratory International Progress Report IPR-01-57.

Cooper, H.H. JR. & Jacob, C.E., 1946: A Generalized Graphical Method for Evaluating Formation Constants and Summarizing Well-Field History. - Am. Geophys. Union Trans., Vol. 27, No. 4, pp. 526-534.

Doe, T.,1999: Reconciliation of the March'99 Structural model and hydraulic data. Äspö Hard Rock Laboratory. International Progress Report IPR-01-53.

Gentzschein, B and Morosini, M, 1998: TRUE Block Scale Project, Selective Pressure Build-up Tests in Borehole KI0025F. Äspö Hard Rock Laboratory International Progress Report IPR-01-45.

Hantush, M.S. and Jacob, C.E., 1955: Non-steady radial flow in an infinite leaky aquifer. Am. Geophys. Union Trans., vol.36, pp.95-100.

Hermanson J, 1999: TRUE Block Scale Project. Structural model March 1999, based on borehole data from KI0025F02, KA3600F and KA3573A. SKB Internal Report.

Moye, D.G., 1967: Diamond Drilling for Foundation Exploration. Civil Eng. Trans., Inst. Eng. Australia, Apr. 1967, pp. 95-100.

Rouhiainen, P. and Heikkinen, P., 1999: Difference flow measurement in borehole KI0025F03 at the Äspö HRL. International Progress Report IPR-01-55.

Theis, C.V., 1935: The Relationship Between the Lowering of the Piezometric Surface and the Rate and Duration of Discharge Using Ground-Water Storage. - Trans., Amer. Geophys. Union, Vol. 16, pp. 519-524.
.

APPENDIX 1

Description of test diagrams produced by the UHT 1-system.

A flow and pressure build-up test with the UHT 1-equipment comprises 7 stages:

Stage 0: Start of registration
Stage 1: Storing of initial values
Stage 2: Start of packer inflation
Stage 3: Evacuation of air from the pipe string and the measurement hose.
Stage 5: The test valve is closed, the flowing phase is stopped, and the
Stage 6: The recovery ends.
Stage 7: The packers are deflated. Stabilisation of the borehole pressure after the test.

In the two figures below, the variation of the test section pressure (P) and the flow rate (Q) of a typical (outflow-) test are illustrated. The numbers on the x-axis indicate the start of the different stages respectively.

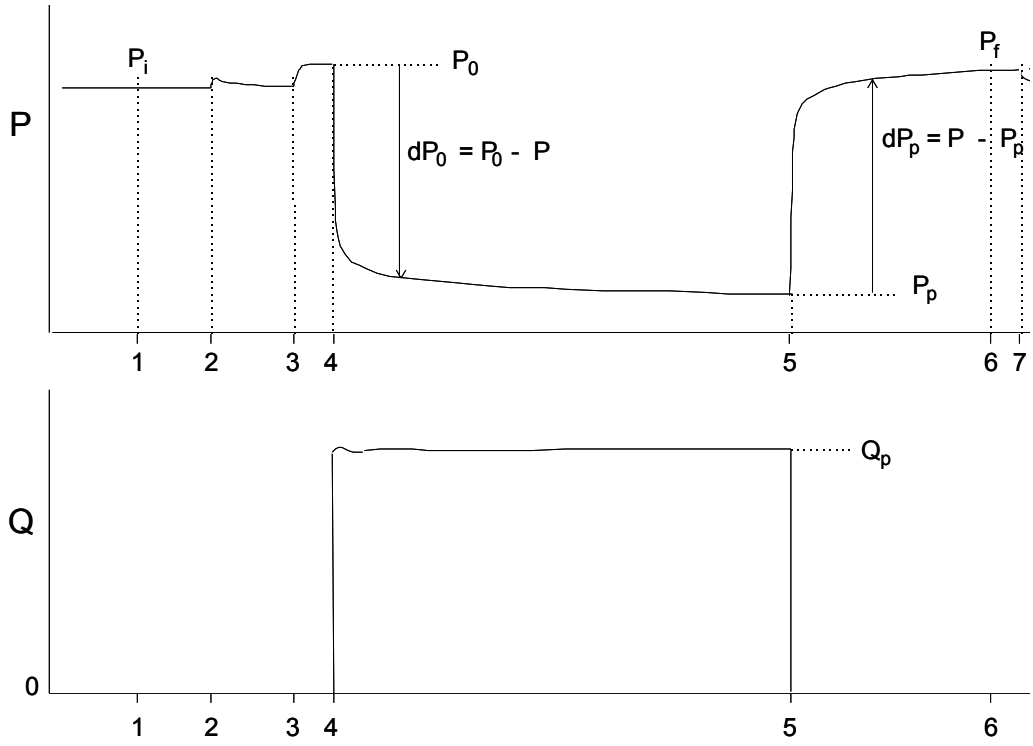

P_i = The first pressure value of stage #1
P_0 = Average of the four last pressure values of stage #3
P_p = Average of the five last pressure values of stage #4 (the last one is excluded)
P_f = The last pressure value of the recovery (stage #5)
Q_p = Average of the five last flow values of stage #4 (the last one is excluded)

A-diagrams show flow-, pressure-, electric conductivity- and temperature variations during the entire test cycle.

A0 A flyleaf showing background data as well as measured and calculated data from the test.

A1
X : Absolute time, stage 0 - 3
Y1: P

A2
X : Absolute time, stage 1 - 7
Y1: Q
Y2: Elcond

A3
X : Absolute time, stage 0 - 7
Y1: P
Y2: Pa
Y3: Pb

A4
X : Absolute time, stage 0 - 7
Y1: Tsec
Y2: Tsurf
Y3: Tair

A5
X : Absolute time, stage 0 - 7
Y1: Ppack
Y2: Pair
Y3: W

B-diagrams show test parameter variations during the flowing phase (stage 4).

B1
X : log (t)
Y1: P
Y2: Tsec
Y3: Elcond

B2
X : $t^{¼}$ and t
Y1: 1/Q

B3
X : $t^{1/2}$ and t
Y1: 1/Q

B4
X : log (t)
Y1: 1/Q
Y2: der(1/Q)

B5
X : log (t)
Y1: log (Q)
Y2: log(der(1/Q))

B6
X : $t^{1/2}$ and t
Y1: Q

C-diagrams show test parameter variations during the recovery phase (stage 5).

C1
X : $t^{¼}$ and dt
Y1: P

C2
X : $t^{1/2}$ and dt
Y1: P

C3
X : $(tpp + dt)^{1/2} - dt^{½}$ and dt
Y1: P

C4
X : log(dt) and dt
Y1: P
Y2: der(P)

	Y3:	Q
C5	X :	log(dt/ (tp+dt)) and dt
	Y1:	P
	Y2:	Tsec
C6	X :	log(dte) and dt
	Y1:	log(P-Pp)
	Y2:	log(der(P-Pp))
C7	X :	$(1/dt)^{1/2}$ - $(1/(tpp+dt))^{1/2}$ and dt
	Y1:	P
C8	X :	log(dt)
	Y1:	P
	Y2:	der(P)
	Y3:	Q
C9	X :	log(dt)
	Y1:	log(P-Pp)
	Y2:	log(der(P-Pp))

Symbols and calculations of the UHT 1 diagrams

Symbols

TT	Test type
DW	Borehole diameter
X	x-coordinate, top of casing
Y	y-coordinate, top of casing
Z	altitude, top of casing
AW	Borehole azimut
IW	Borehole inclination
TC	Test crew
EC	Equipment code
TB	Time (YYMMDDhhmmss) when PB and BB are measured
PB	Barometric pressure at time TB (measured by P-the test section sensor)
BB	Barometric pressure at time TB (measured by Pair, not in use)
tabs	time
t	elapsed time from pump start
dt	elapsed time from pump stop
tp	duration of flow phase
tpp	corrected tp
dte	equivalent time
dtf	duration of the pressure recovery
Vtot	total flowing volume during the flowing phase
Crit 4	criteria of the start of the flow phase
Difft 4	the start time of the flow phase is set “Difft 4” seconds before (negative) or after (positive) the time point when the criteria Crit4 is accomplished.
Crit 5	criteria of the start of the recovery period
Difft 5	the start time of the recovery period is set “Difft 5” seconds before (negative) or after (positive) the time point when the criteria Crit5 is accomplished

tdiffstart time difference between the time, when the data processing system is initiated to begin the flow phase and the time when the flow phase really starts according to the criteria Crit 4.

tdiffstop time difference between the time, when the data processing system is initiated to begin the recovery period and the time when the recovery period really starts according to the criteria Crit 5.

dl4 Smoothing for derivative calculations, flow phase

dl5 Smoothing for derivative calculations, recovery phase

Crit 4, Difft 4, Crit 5, Difft 5, dl4 and dl5 are input values to the plot program IPPLOT:

Measured variables

P ground-water pressure of the test section

P_a ground-water pressure of the borehole interval below the test section

P_b ground-water pressure of the test section

P_{pack} Packer-pressure

P_w Pressure of the ground-water level sensor (not in use)

Q2 flow rate of the big flow meter (Qbig)

Q1 flow rate of the small flow meter (Q_{small})

Q Flow rate from the test section, one of Q1 or Q2. It is not possible to know which one of Q_{small} or Qbig that is used unless you study the data file *.HT2

Tsec Temperature of the test section (not in use)

Tsurf Temperature of the injection water at surface.

Tair Air temperature in the measurement container (not in use)

Pair Barometric pressure (not in use)

W Ground-water level (not in use)

Calculations

Vtot = the integral of the flow rate (Q) during the flowing phase (stage 4)
All values are integrated, the negative values as well.

tpp = (Vtot/Qp) or = tp.

dte = dt * tp/ (dt + tp)

From the variables P, P_a, P_b, W and Q constants, with indices i, o, p, f and e, are determined according to:

i The first value of stage 1

o Average of the 4 last values of stage 3.

p Average of the 5 last values of stage 4, excluding the last value.

f The last value of stage 5

e The last value of stage 7

Transformation of the pressure values in the diagrams have been carried out according to:

P (diagram) = P (measured) + LK * sin(IW) * 9.807
P_a (diagram) = P_a (measured) + LM * sin(IW) * 9.807
P_b(diagram) = P_b (measured) + LK * sin(IW) * 9.807

LK, LM = Distance from the pressure transducers to the top of the test section.

dP_{im} Average of differential pressure ($P - P_i$) during the flow phase (stage 4) with the open hole pressure (P_i) as a reference.

dP_{om} Average of differential pressure ($P - P_o$) during the flow phase (stage 4) with the section pressure before the flow start(P_o) as a reference.

$$Koss = \frac{Qp \times 1000 \times 9.81}{L \times dP_{om}} \cdot [1 + \ln(L/2r_w)]/ 2\pi$$

L = Length of the test section (m)
r_w = borehole radius (m)

$$Kiss = \frac{Qp \times 1000 \times 9.81}{L \times dP_{im}} \cdot [1 + \ln(L/2r_w)]/ 2\pi$$

L = Length of the test section (m)

APPENDIX 2: Diagrams of the Selective Pressure Build-up Tests in KI0025F03

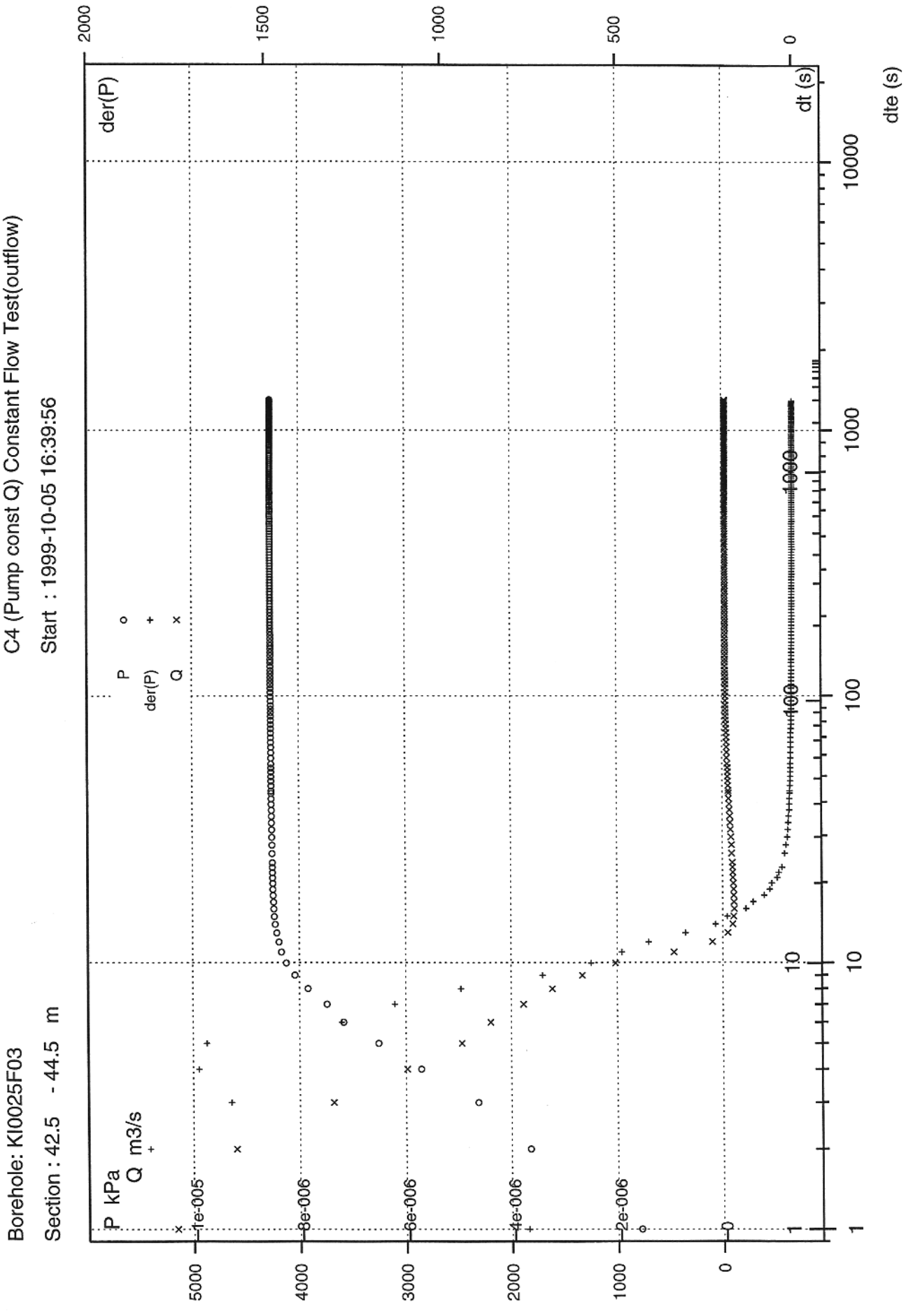
Borehole: KI0025F03
Section : 42.5 - 44.5 m
C4 (Pump const Q) Constant Flow Test(outflow)
Start : 1999-10-05 16:39:56
P kPa
Q m3/s
der(P)
dt (s)
dte (s)
P
der(P)
Q

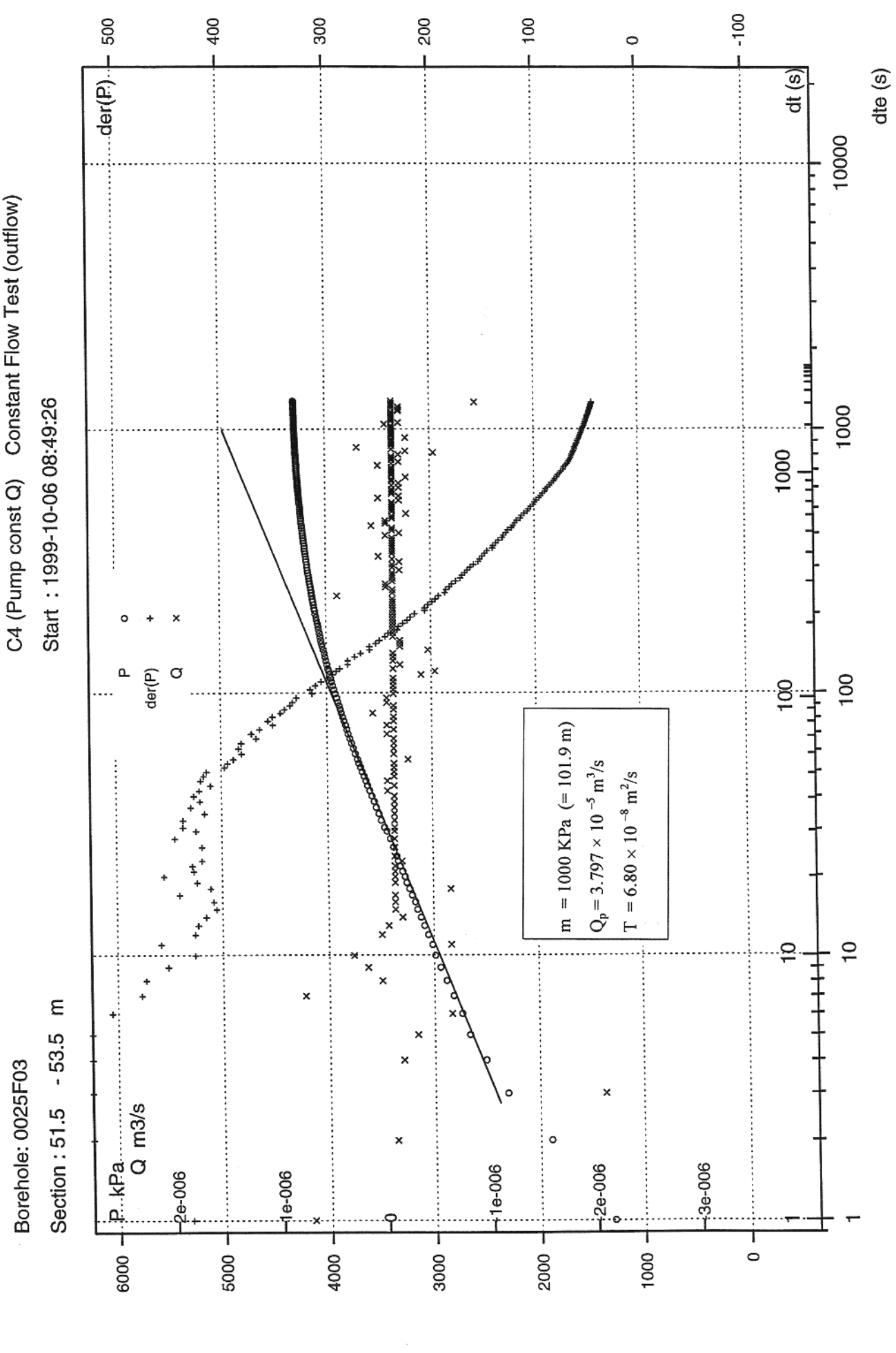
C4 (Pump const Q) Constant Flow Test (outflow)
Start : 1999-10-06 08:49:26
Borehole: 0025F03
Section : 51.5 - 53.5 m
P kPa
Q m3/s
der(P)
dt (s)
dte (s)
P
der(P)
Q
m = 1000 KPa (= 101.9 m)
$Q_p = 3.797 \times 10^{-5}$ m^3/s
$T = 6.80 \times 10^{-8}$ m^2/s

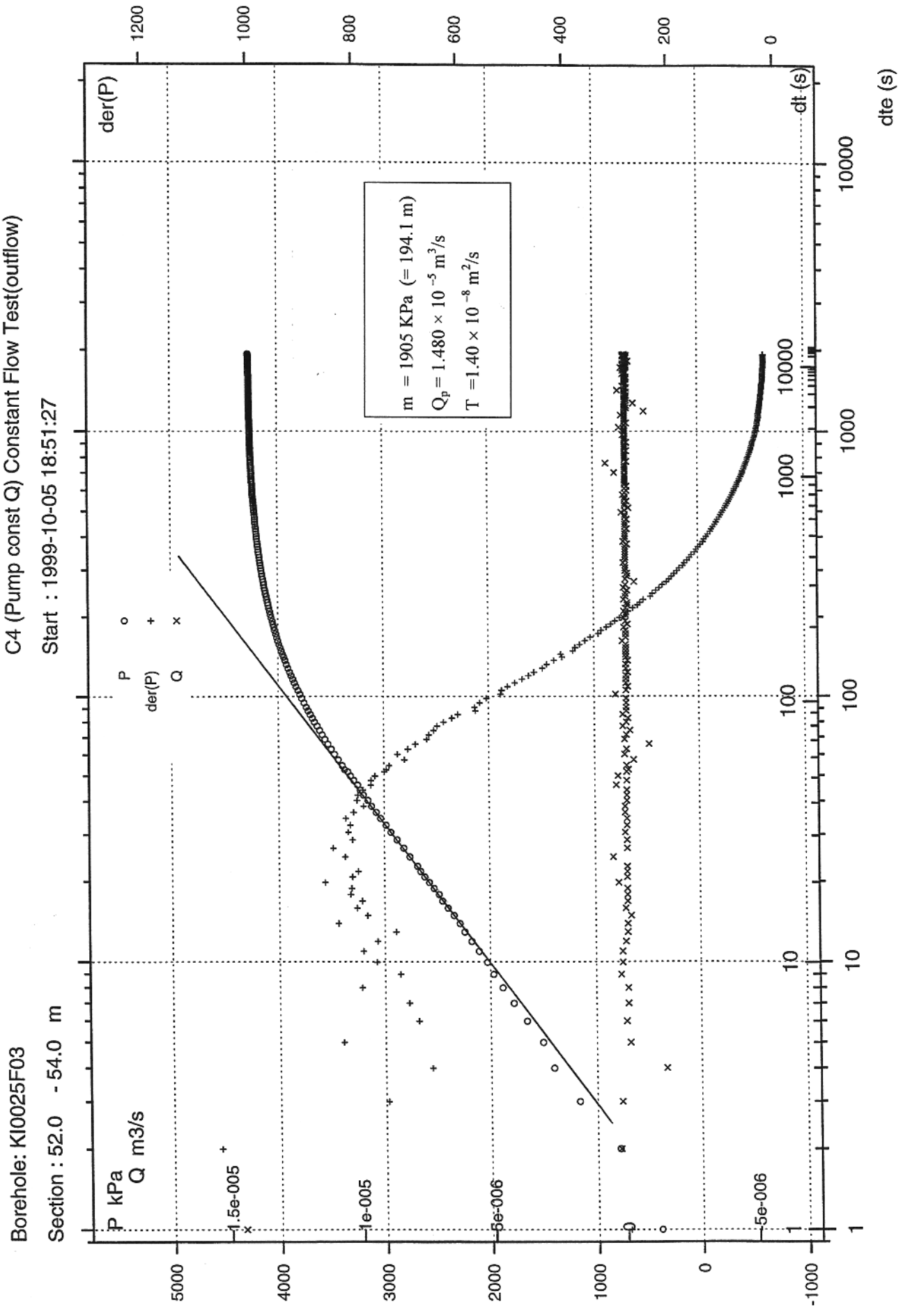
Borehole: KI0025F03
Section : 52.0 - 54.0 m
C4 (Pump const Q) Constant Flow Test(outflow)
Start : 1999-10-05 18:51:27
P kPa
Q m3/s
der(P)
dt (s)
dte (s)
P
der(P)
Q
m = 1905 KPa (= 194.1 m)
Q_p = 1.480 × 10 $^{-5}$ m^3/s
T =1.40 × 10 $^{-8}$ m^2/s

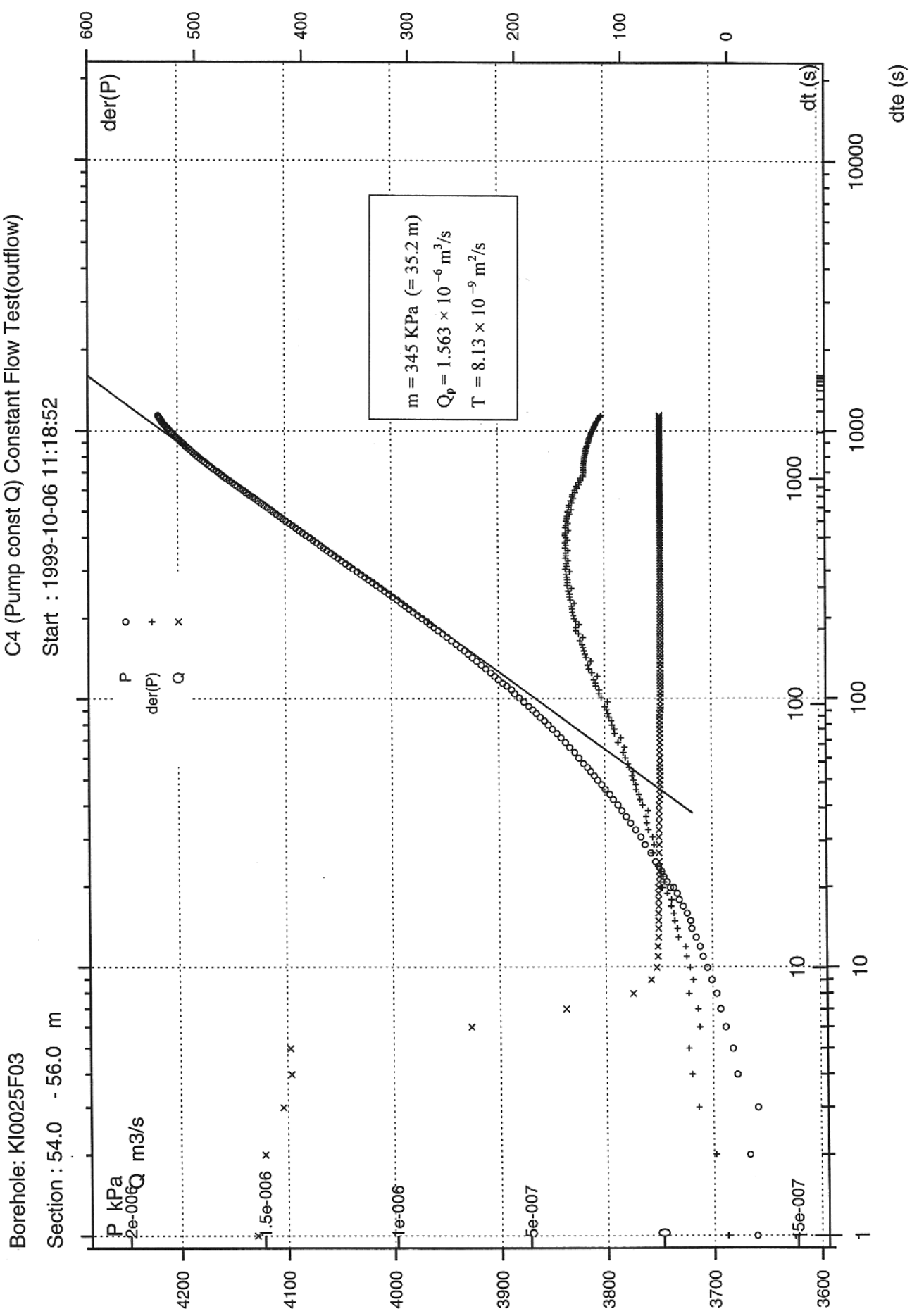
Borehole: KI0025F03
Section : 54.0 - 56.0 m
C4 (Pump const Q) Constant Flow Test(outflow)
Start : 1999-10-06 11:18:52
P kPa
Q m3/s
der(P)
dt (s)
dte (s)
P
der(P)
Q
m = 345 KPa (= 35.2 m)
$Q_\rho = 1.563 \times 10^{-6}$ m^3/s
$T = 8.13 \times 10^{-9}$ m^2/s

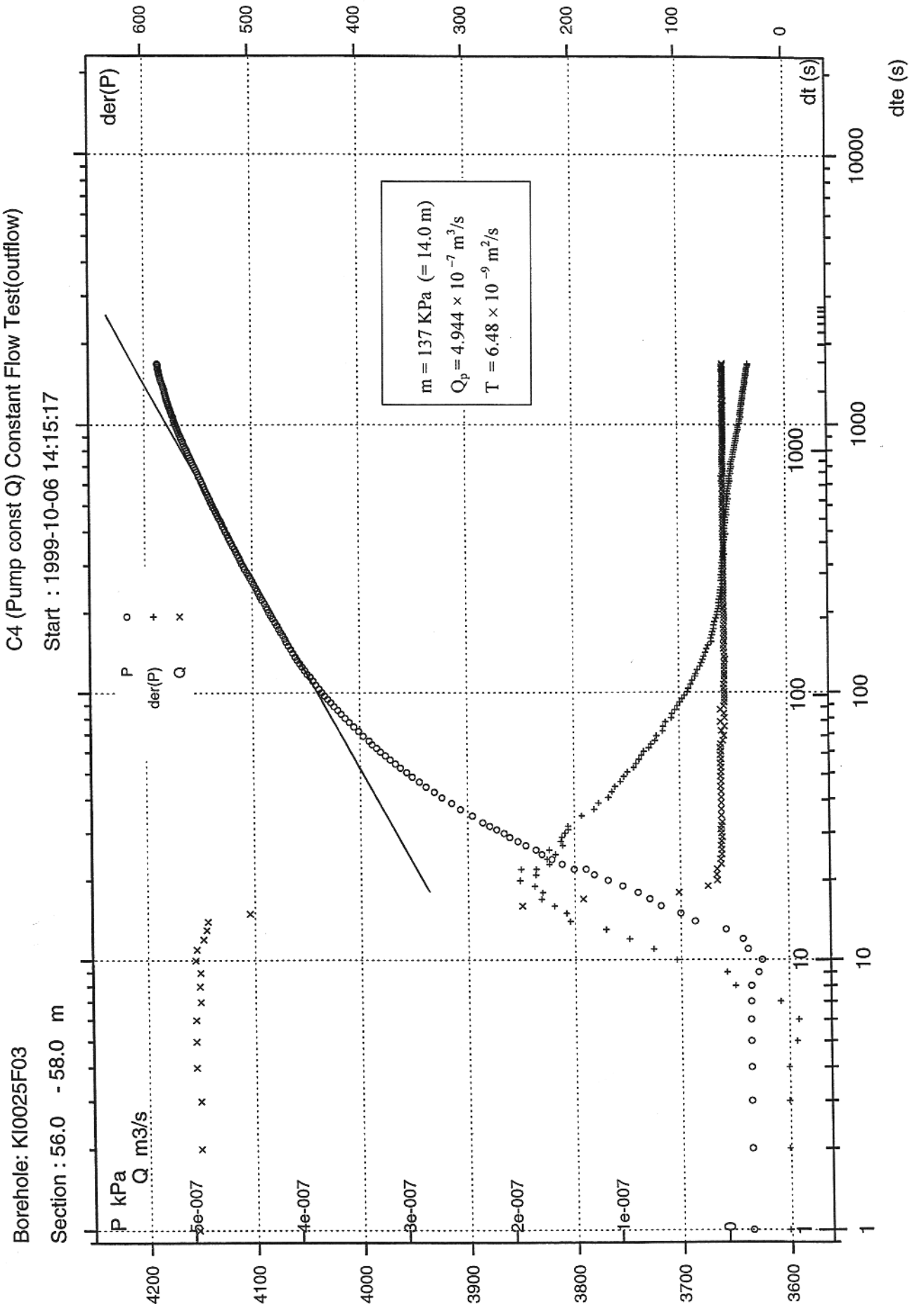
C4 (Pump const Q) Constant Flow Test(outflow)
Start : 1999-10-06 14:15:17
Borehole: KI0025F03
Section : 56.0 - 58.0 m
P kPa
Q m3/s
der(P)
dt (s)
dte (s)
P
der(P)
Q
m = 137 KPa (= 14.0 m)
$Q_p = 4.944 \times 10^{-7}$ m^3/s
$T = 6.48 \times 10^{-9}$ m^2/s

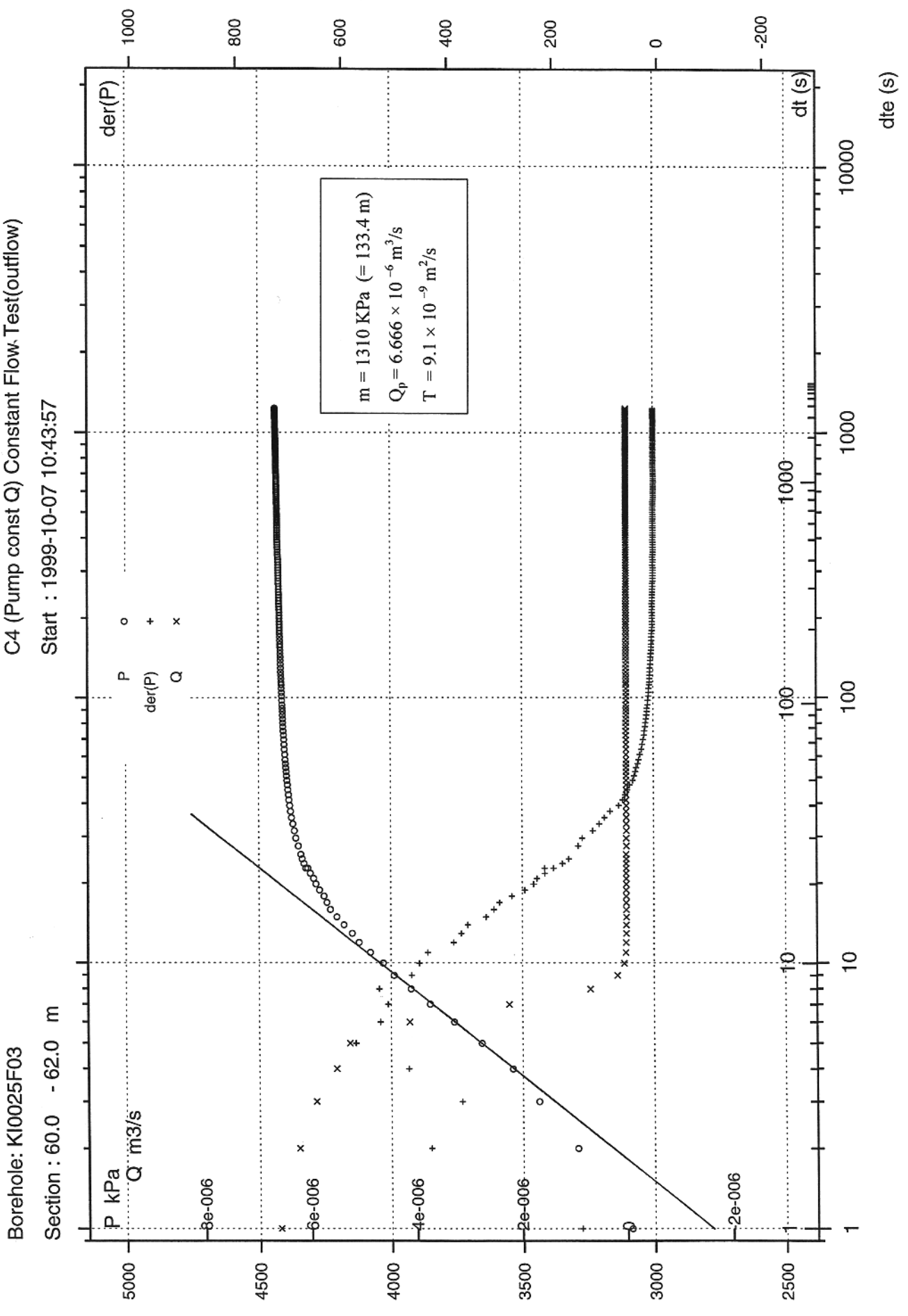
Borehole: KI0025F03
Section : 60.0 - 62.0 m
C4 (Pump const Q) Constant Flow-Test(outflow)
Start : 1999-10-07 10:43:57
P kPa
Q m3/s
der(P)
dt (s)
dte (s)
P
der(P)
Q
m = 1310 KPa (= 133.4 m)
$Q_p = 6.666 \times 10^{-6}$ m³/s
$T = 9.1 \times 10^{-9}$ m²/s

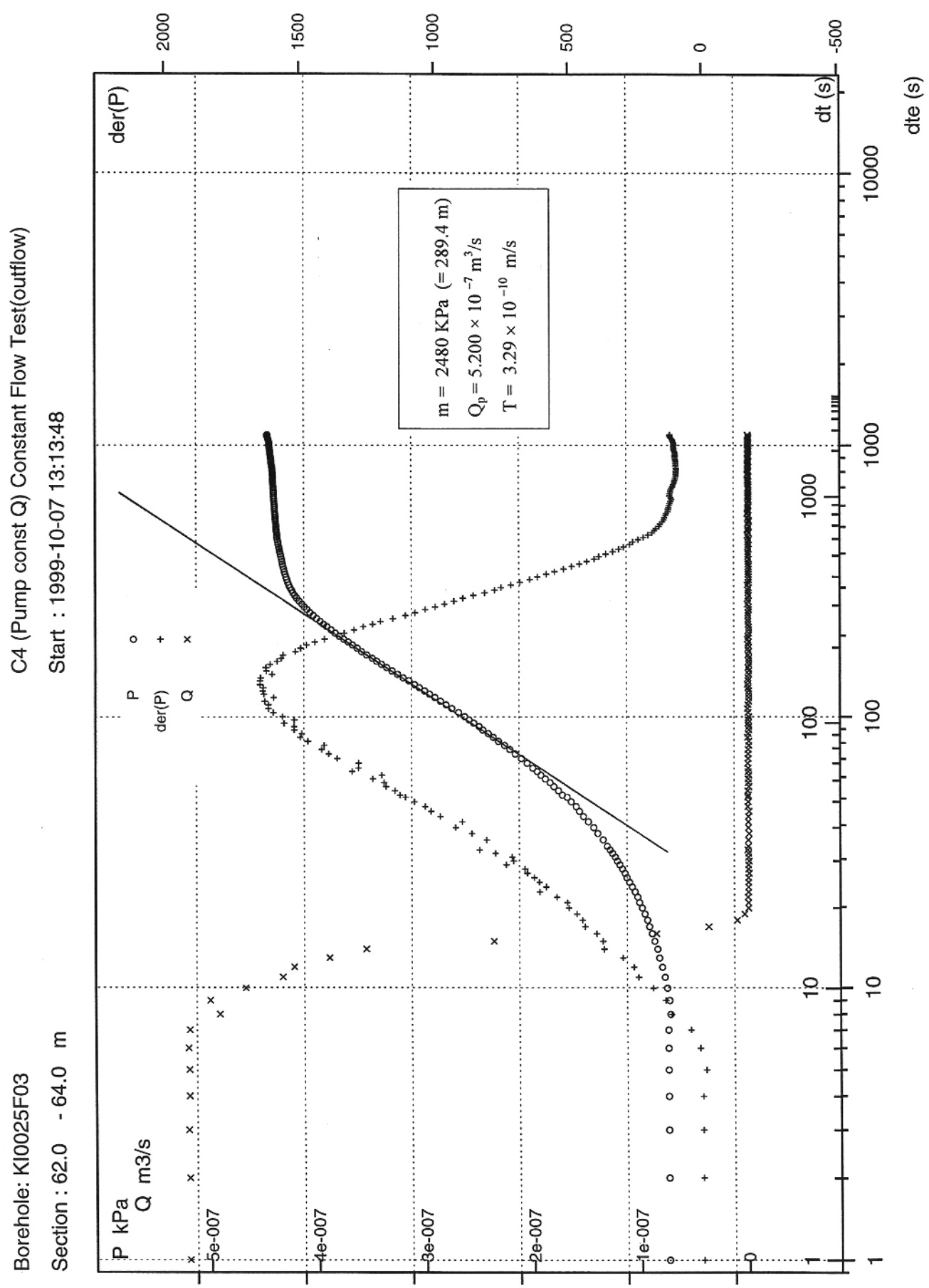
Borehole: KI0025F03
Section : 62.0 - 64.0 m
C4 (Pump const Q) Constant Flow Test(outflow)
Start : 1999-10-07 13:13:48
P kPa
Q m3/s
der(P)
dt (s)
dte (s)
P
der(P)
Q
m = 2480 KPa (= 289.4 m)
$Q_p = 5.200 \times 10^{-7}$ m^3/s
T = 3.29×10^{-10} m/s

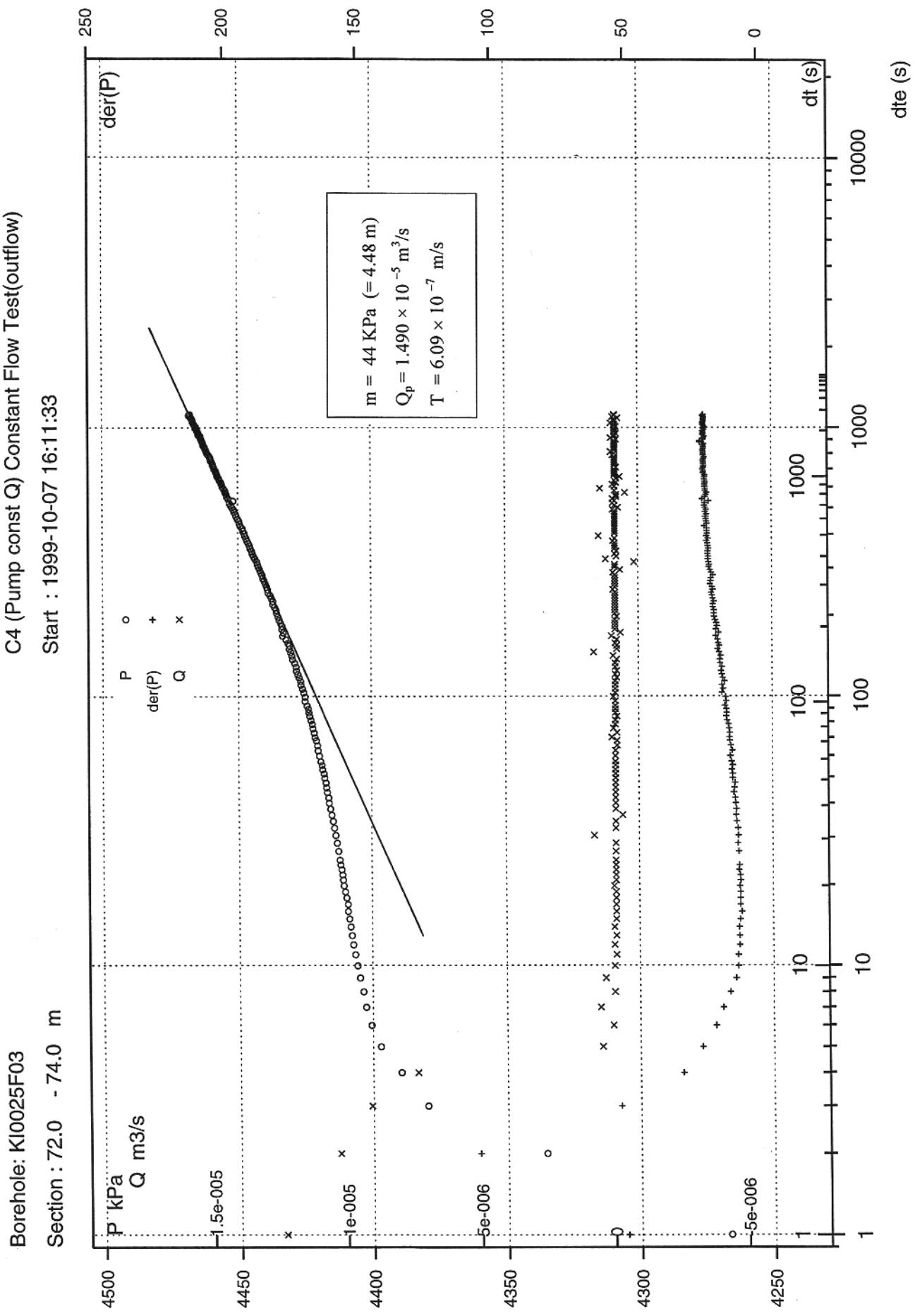
Borehole: KI0025F03
Section : 72.0 - 74.0 m
C4 (Pump const Q) Constant Flow Test(outflow)
Start : 1999-10-07 16:11:33
P kPa
Q m3/s
der(P)
dt (s)
dte (s)
P
der(P)
Q
m = 44 KPa (= 4.48 m)
$Q_p = 1.490 \times 10^{-5}$ m^3/s
$T = 6.09 \times 10^{-7}$ m/s

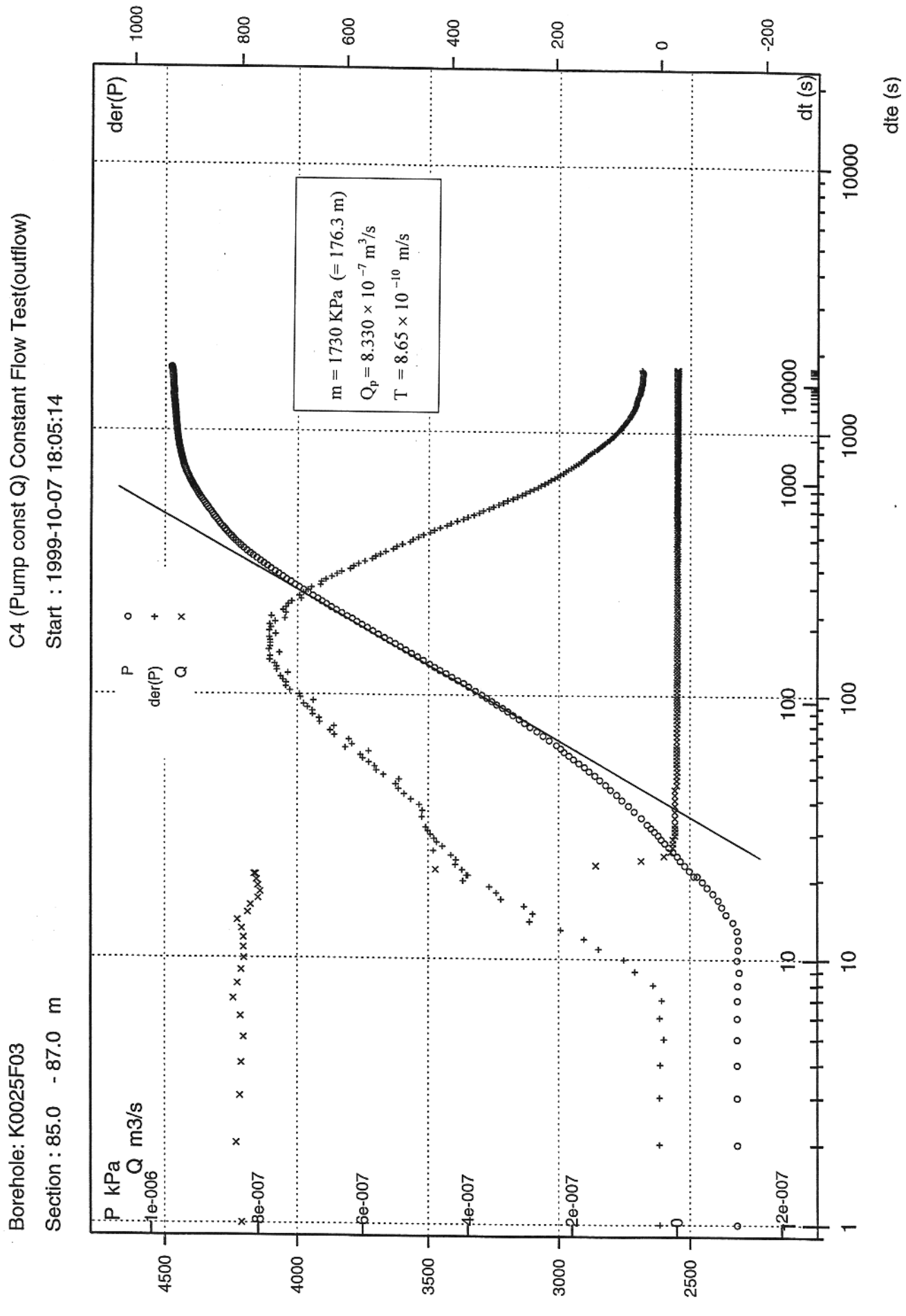
Borehole: K0025F03
Section : 85.0 - 87.0 m
C4 (Pump const Q) Constant Flow Test(outflow)
Start : 1999-10-07 18:05:14
P kPa
Q m3/s
der(P)
dt (s)
dte (s)
P
der(P)
Q
m = 1730 KPa (= 176.3 m)
Q_p = 8.330 × 10 $^{-7}$ m^3/s
T = 8.65 × 10 $^{-10}$ m/s

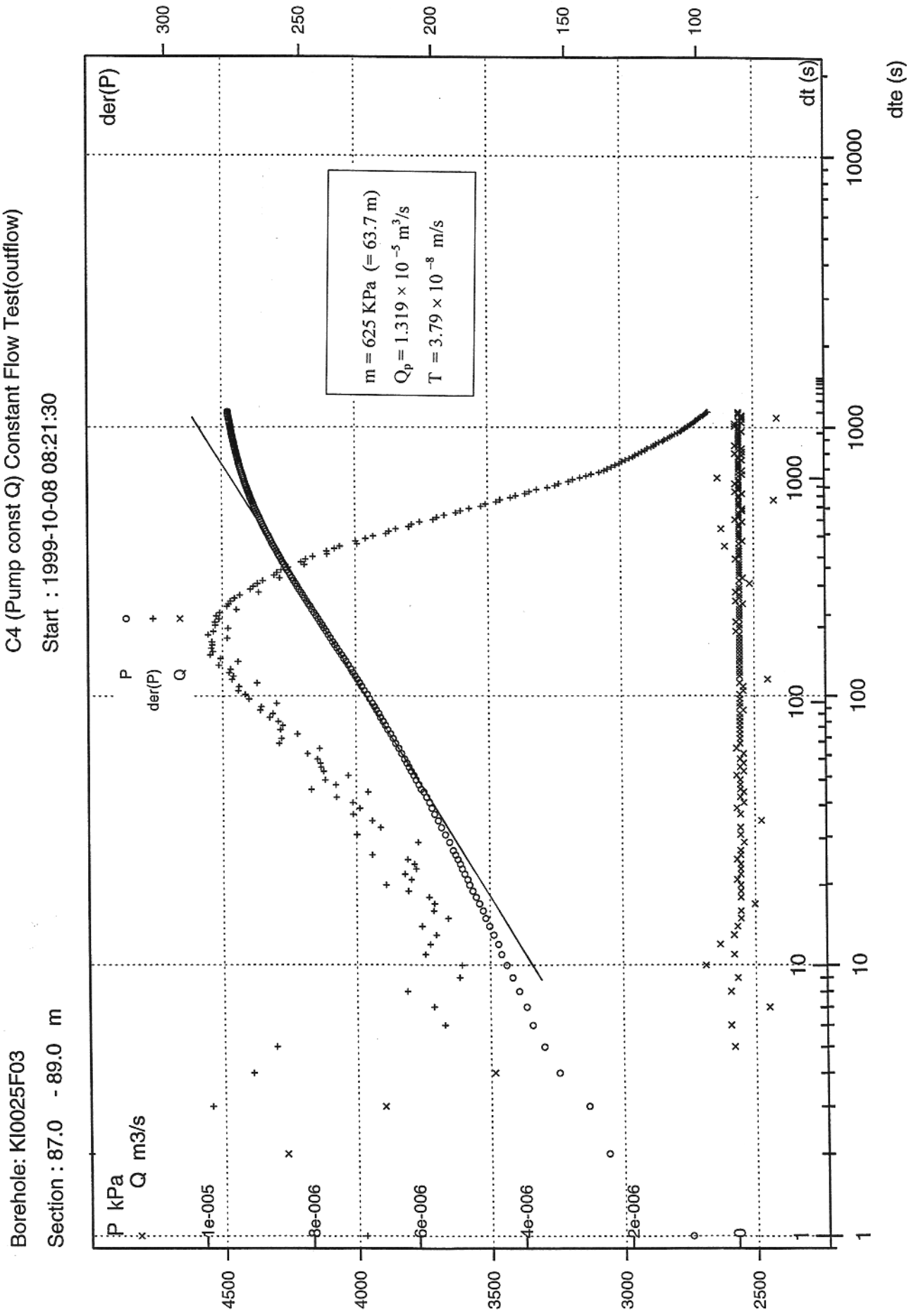
Borehole: KI0025F03
Section : 87.0 - 89.0 m
C4 (Pump const Q) Constant Flow Test(outflow)
Start : 1999-10-08 08:21:30
P kPa
Q m3/s
der(P)
dt (s)
dte (s)
P
der(P)
Q
m = 625 KPa (= 63.7 m)
Qp = 1.319 × 10 -5 m3/s
T = 3.79 × 10 -8 m/s

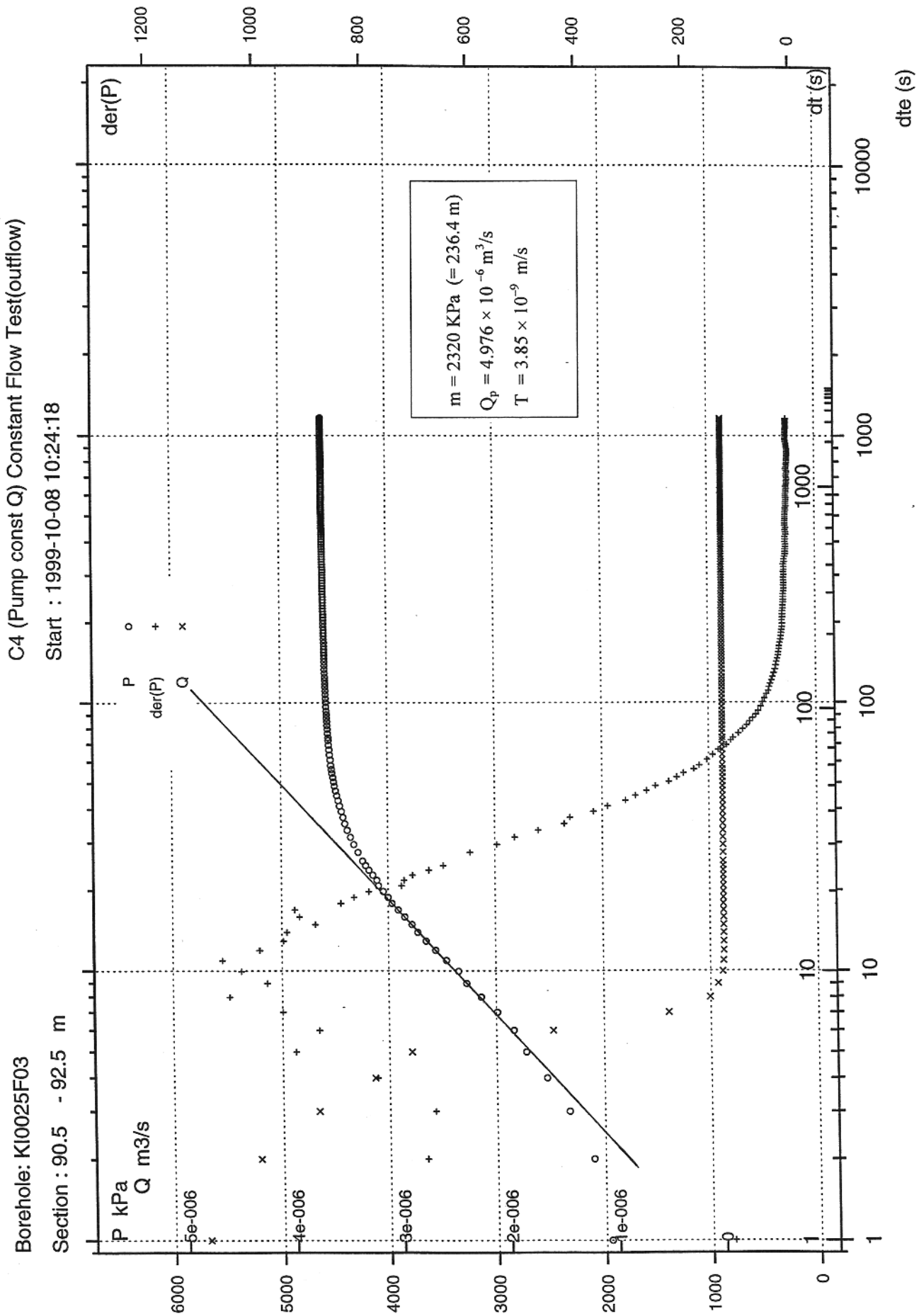
C4 (Pump const Q) Constant Flow Test(outflow)
Borehole: KI0025F03
Section : 90.5 - 92.5 m
Start : 1999-10-08 10:24:18
P kPa
Q m3/s
der(P)
dt (s)
dte (s)
P
der(P)
Q
m = 2320 KPa (= 236.4 m)
$Q_p = 4.976 \times 10^{-6}$ m^3/s
$T = 3.85 \times 10^{-9}$ m/s

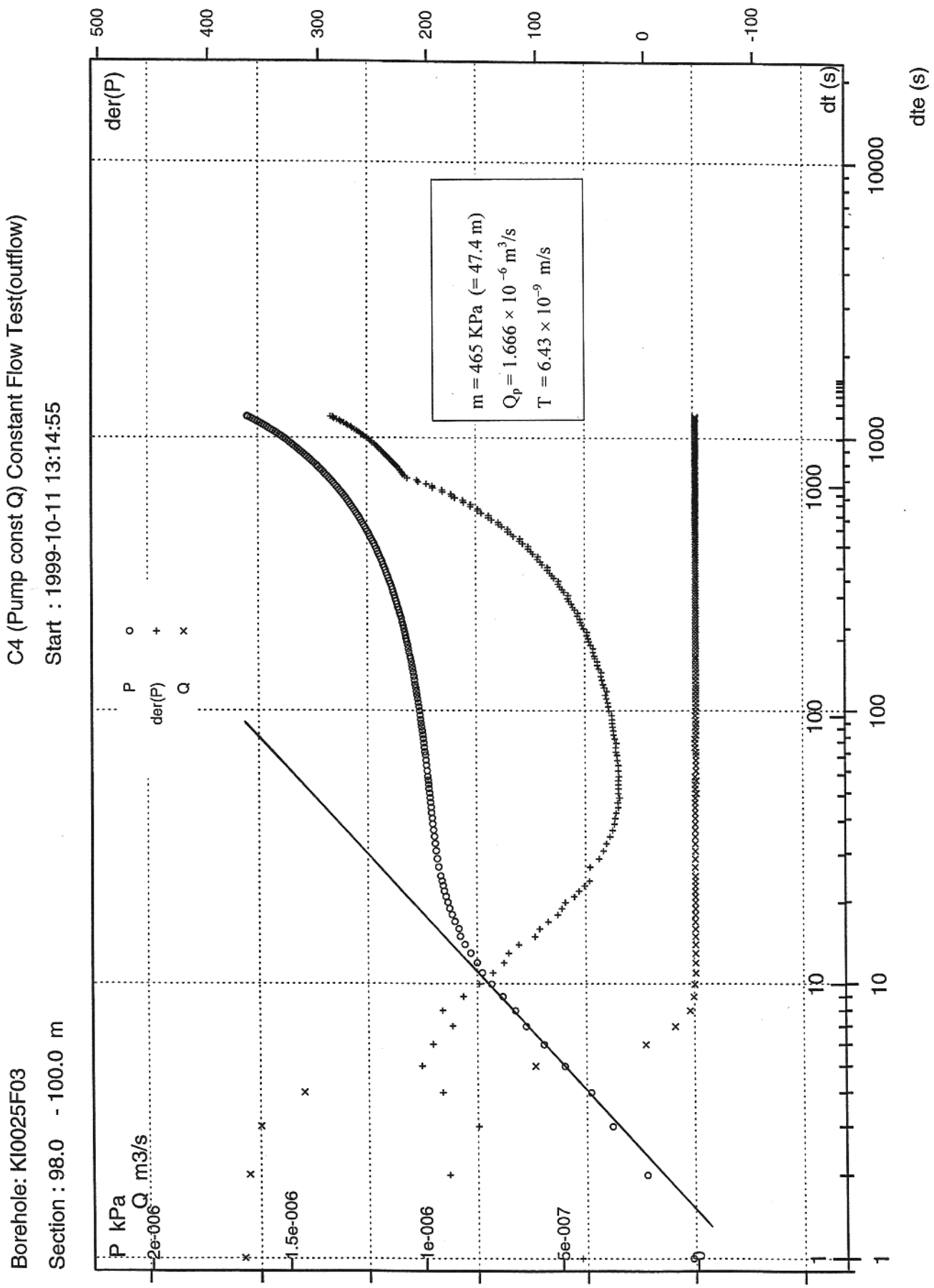
Borehole: KI0025F03
Section : 98.0 - 100.0 m
C4 (Pump const Q) Constant Flow Test(outflow)
Start : 1999-10-11 13:14:55
P kPa
Q m3/s
der(P)
dt (s)
dte (s)
P
der(P)
Q
m = 465 KPa (= 47.4 m)
$Q_p = 1.666 \times 10^{-6}$ m^3/s
$T = 6.43 \times 10^{-9}$ m/s

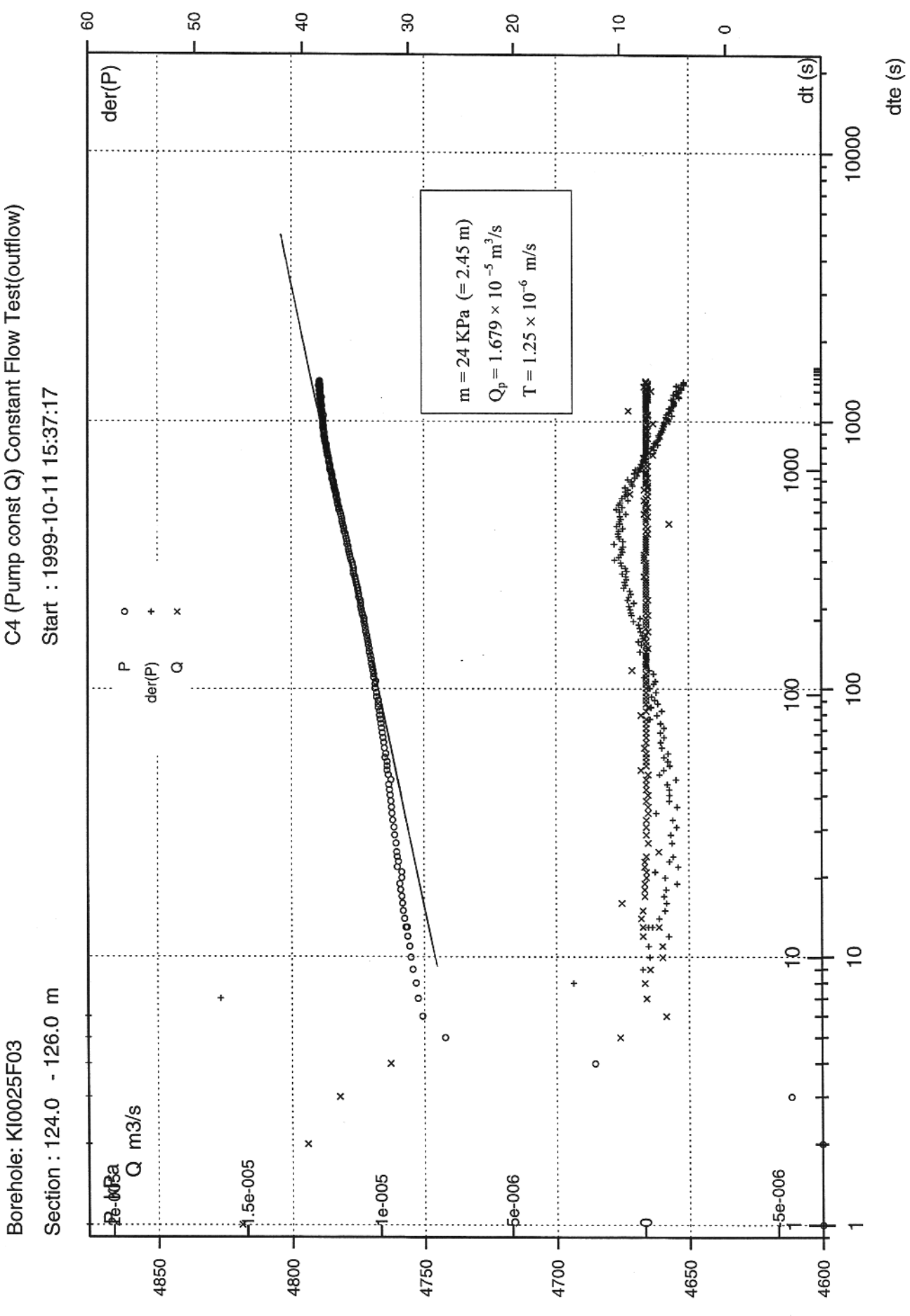
Borehole: KI0025F03
Section : 124.0 - 126.0 m
C4 (Pump const Q) Constant Flow Test(outflow)
Start : 1999-10-11 15:37:17
P
der(P)
Q
der(P)
dt (s)
dte (s)
Q m3/s
m = 24 KPa (= 2.45 m)
$Q_p = 1.679 \times 10^{-5}$ m³/s
$T = 1.25 \times 10^{-6}$ m/s

APPENDIX 3: Pressure response plots from the short-term interference tests in KI0025F03.

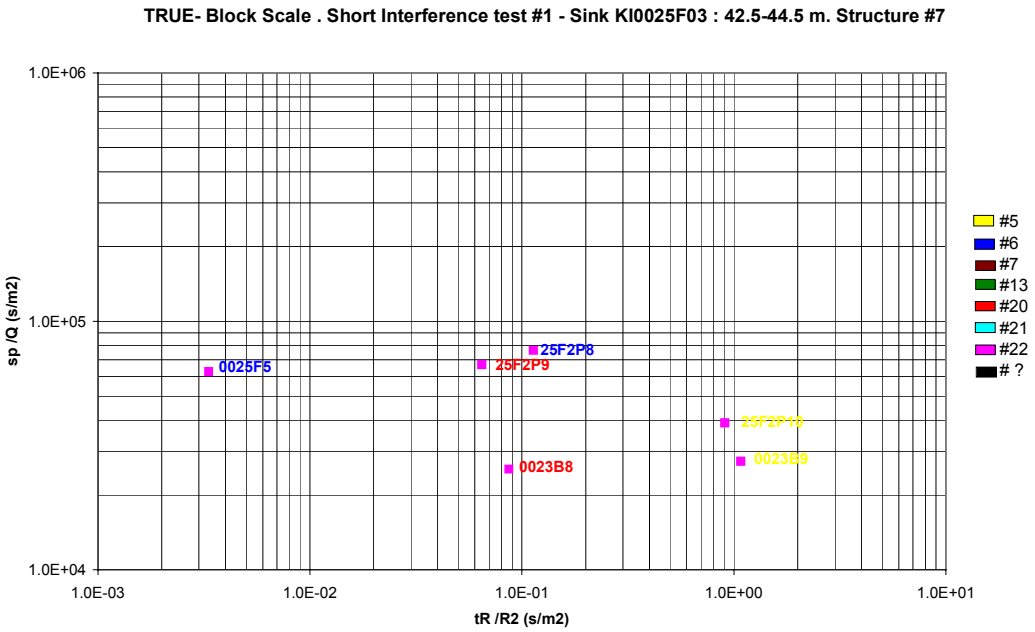

TRUE- Block Scale . Short Interference test #2a - Sink KI0025F03 : 52.0-54.0 m. Structure #6

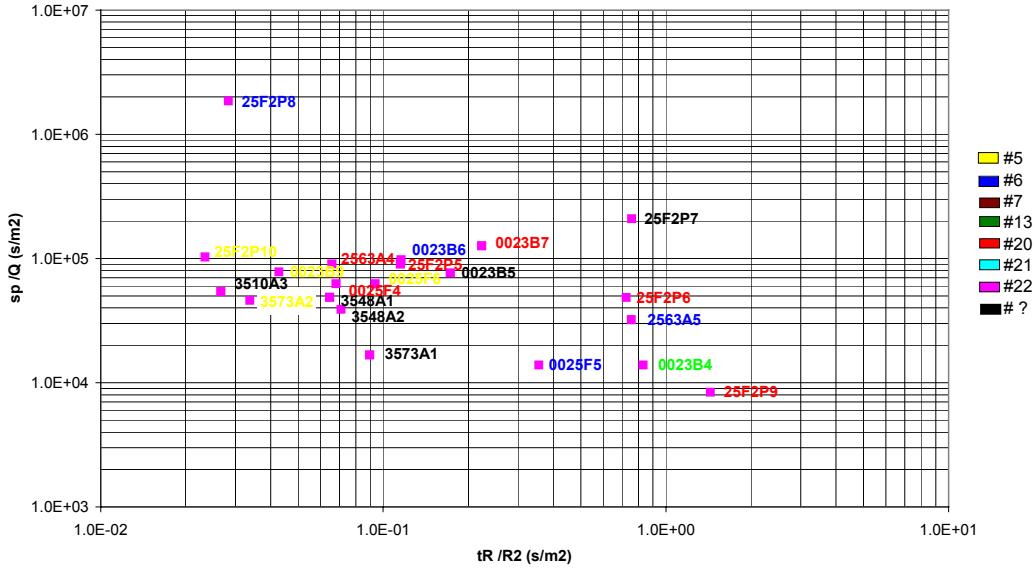

TRUE- Block Scale . Short Interference test #2b - Sink KI0025F03 : 51.5-53.5 m. Structure #6

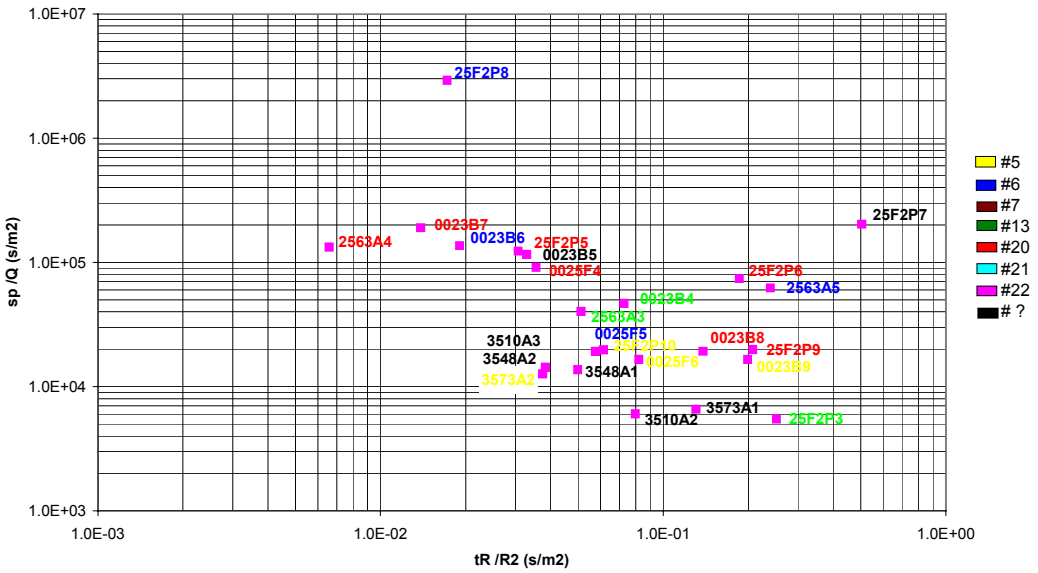

TRUE- Block Scale . Short Interference test #3 - Sink KI0025F03 : 54.0-56.0 m. Structure #?

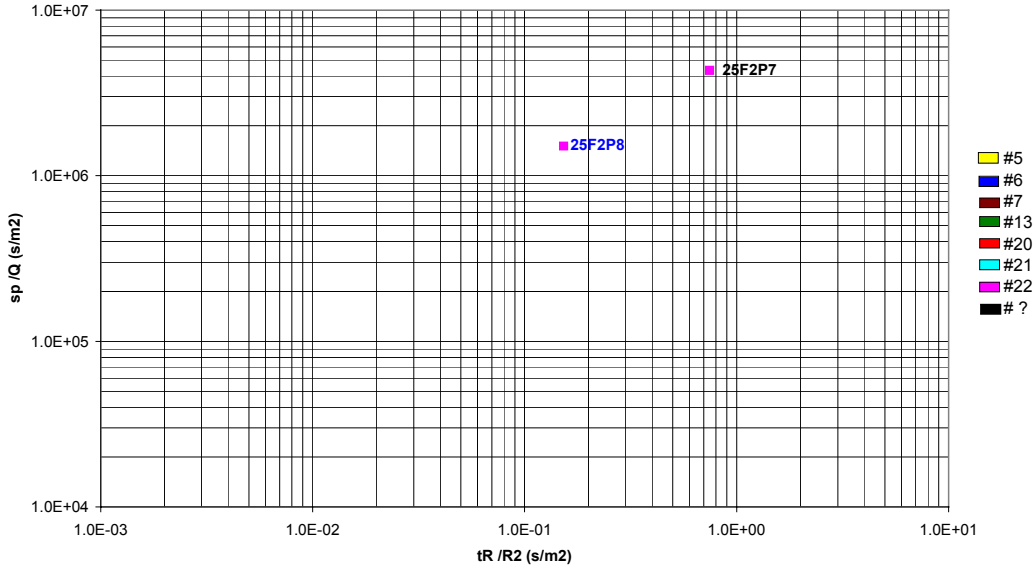

TRUE- Block Scale . Short Interference test #4 - Sink KI0025F03 : 56.0-58.0 m. Structure #?

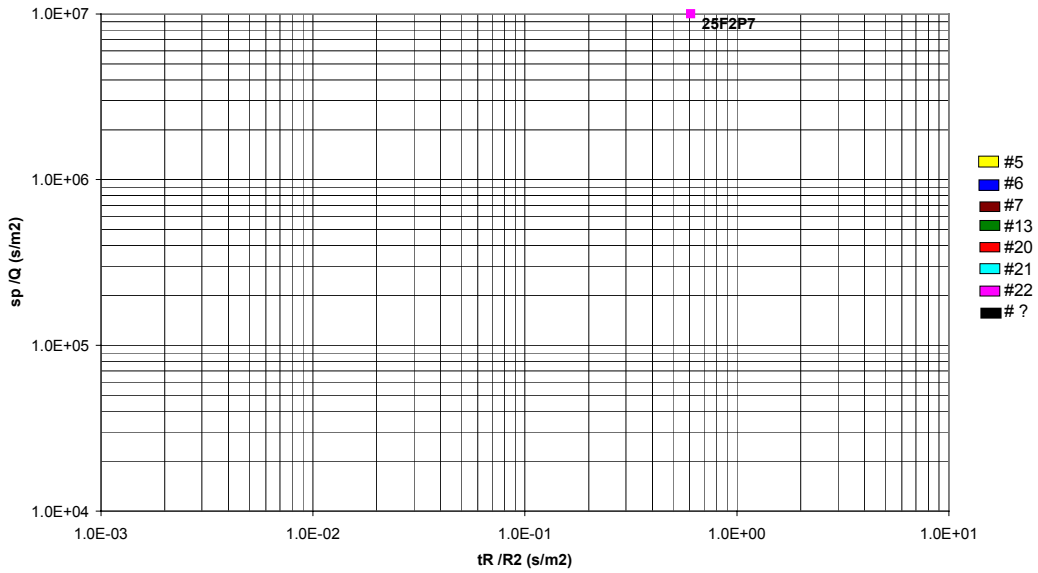

TRUE- Block Scale . Short Interference test #5 - Sink KI0025F03 : 60.0-62.0 m. Structure #22

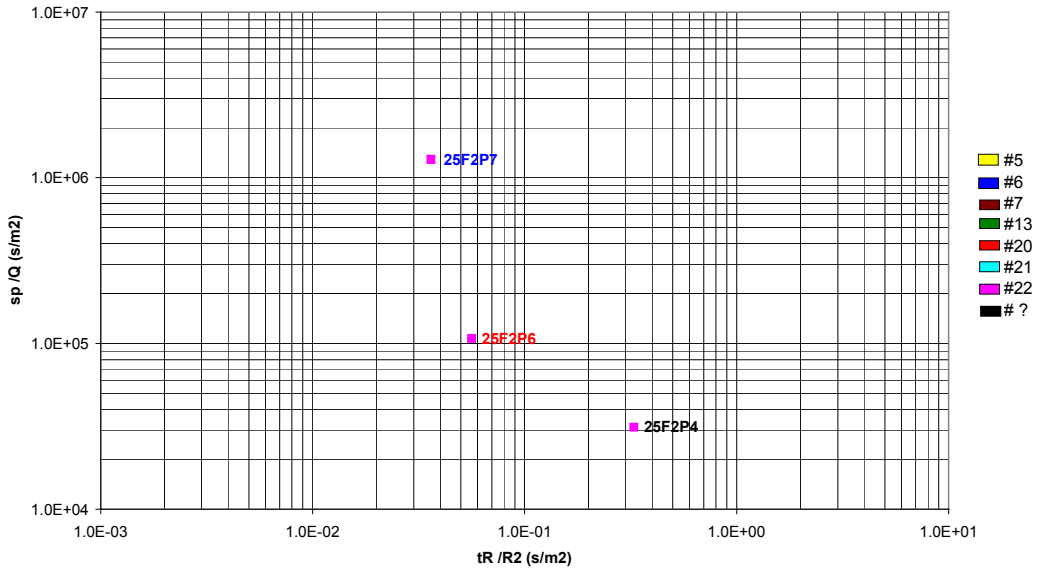

TRUE- Block Scale . Short Interference test #6 - Sink KI0025F03 : 62.0-64.0 m. Structure #?

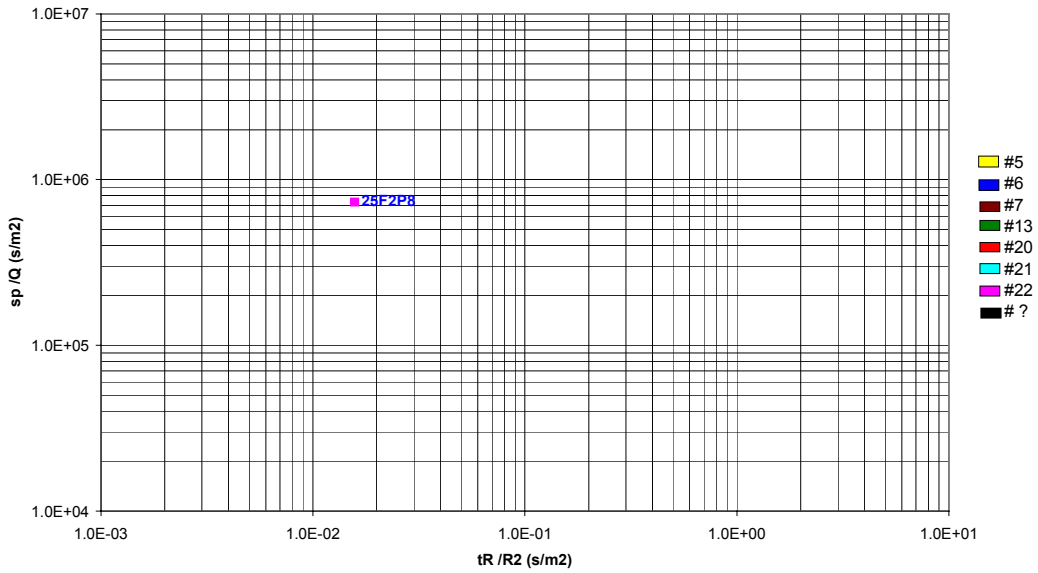

TRUE- Block Scale . Short Interference test #7 - Sink KI0025F03 : 72.0-74.0 m. Structure #20

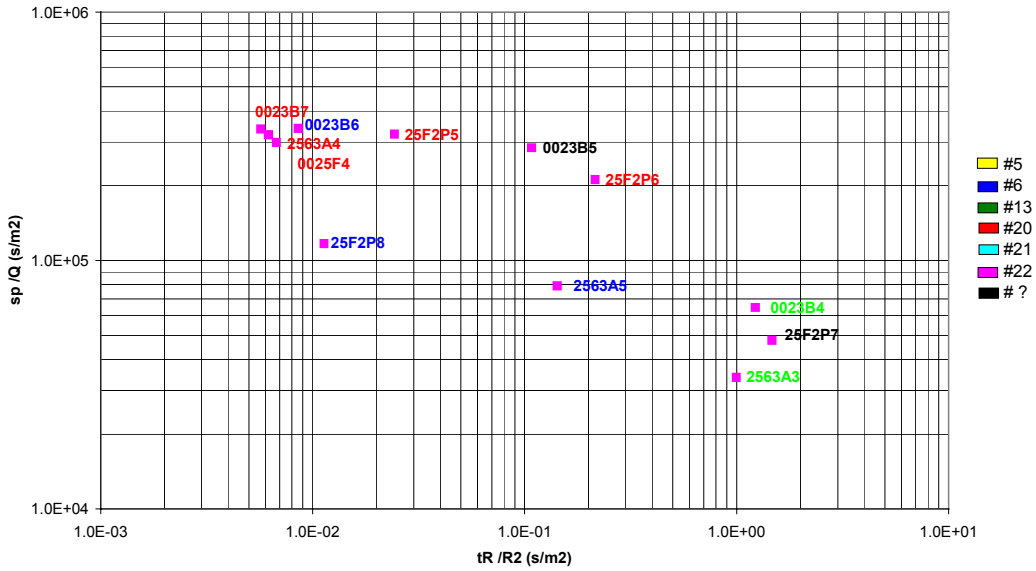

TRUE- Block Scale . Short Interference test #8 - Sink KI0025F03 : 85.0-87.0 m. Structure #?

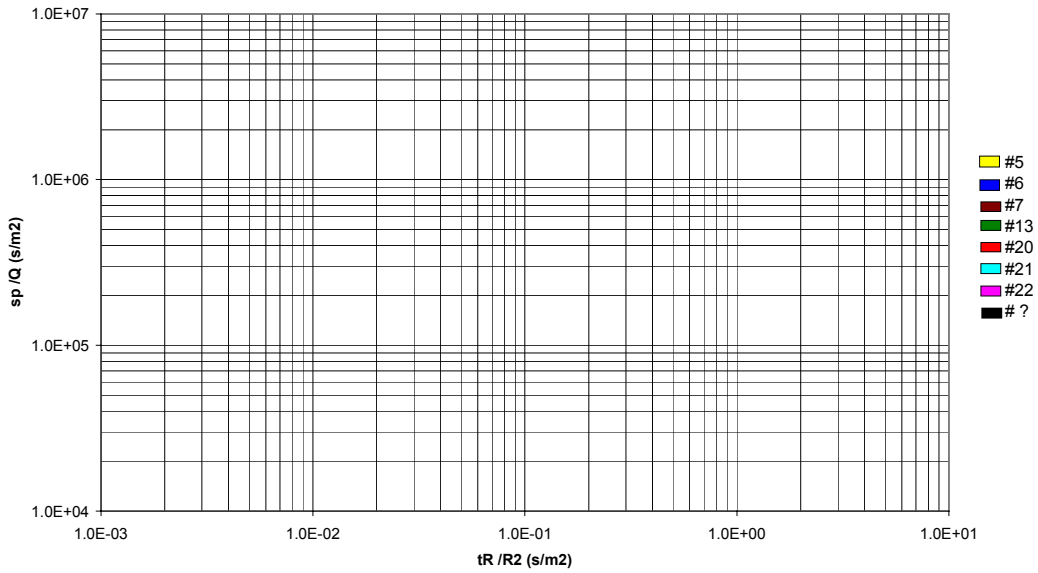

TRUE- Block Scale . Short Interference test #9 - Sink KI0025F03 : 87.0-89.0 m. Structure #21?

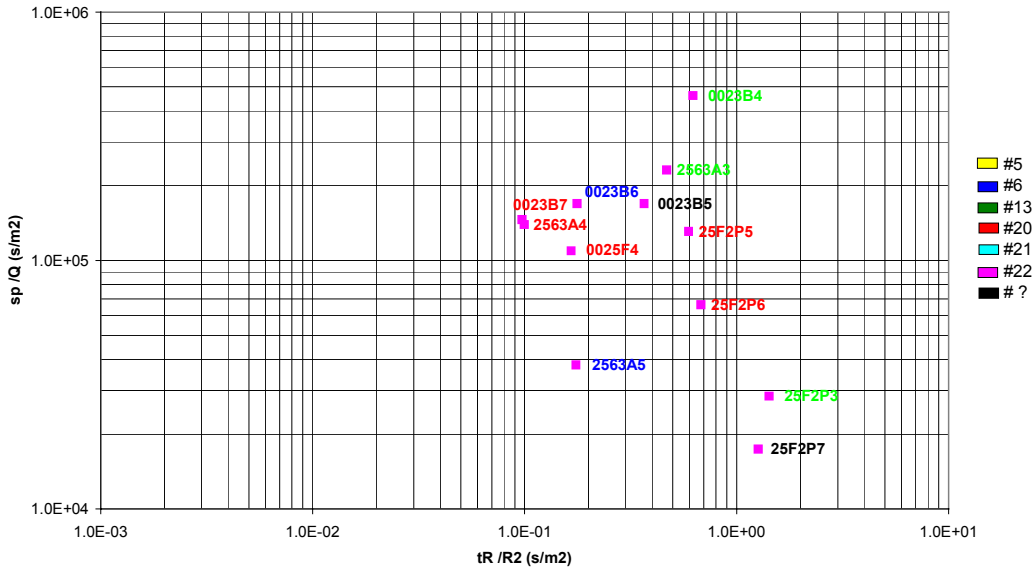

TRUE- Block Scale . Short Interference test #10 - Sink KI0025F03 : 90.5-92.5 m. Structure #13

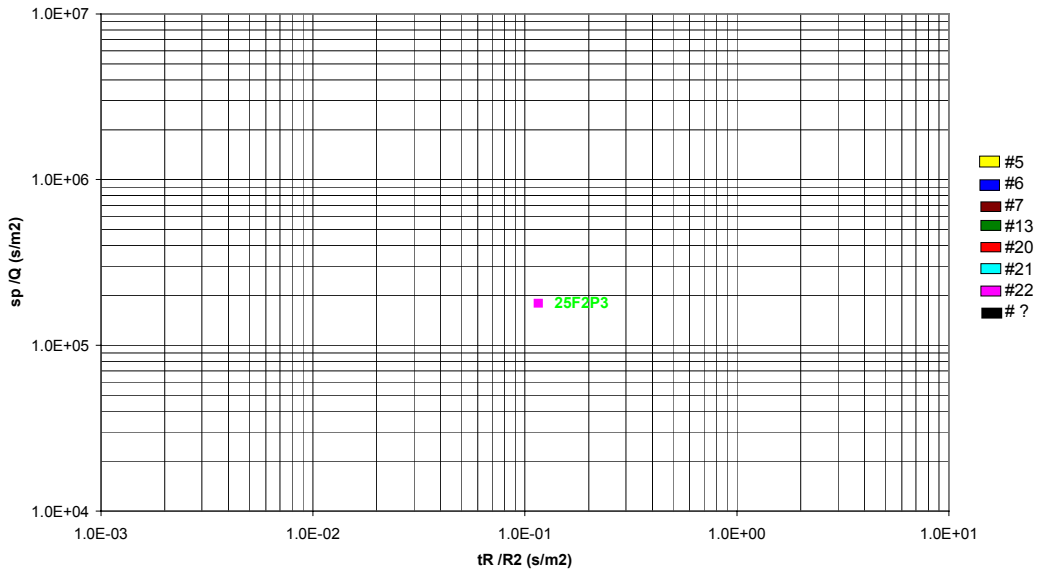

TRUE- Block Scale . Short Interference test #11 - Sink KI0025F03 : 98.0-100.0 m. Structure #?

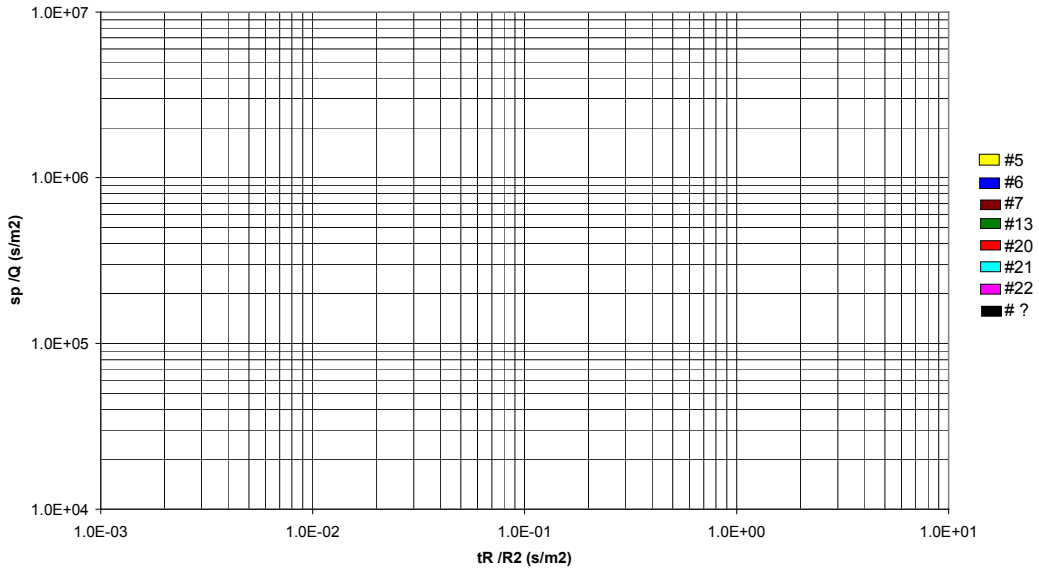

TRUE- Block Scale . Short Interference test #12 - Sink KI0025F03 : 124.0-126.0 m. Structure #19

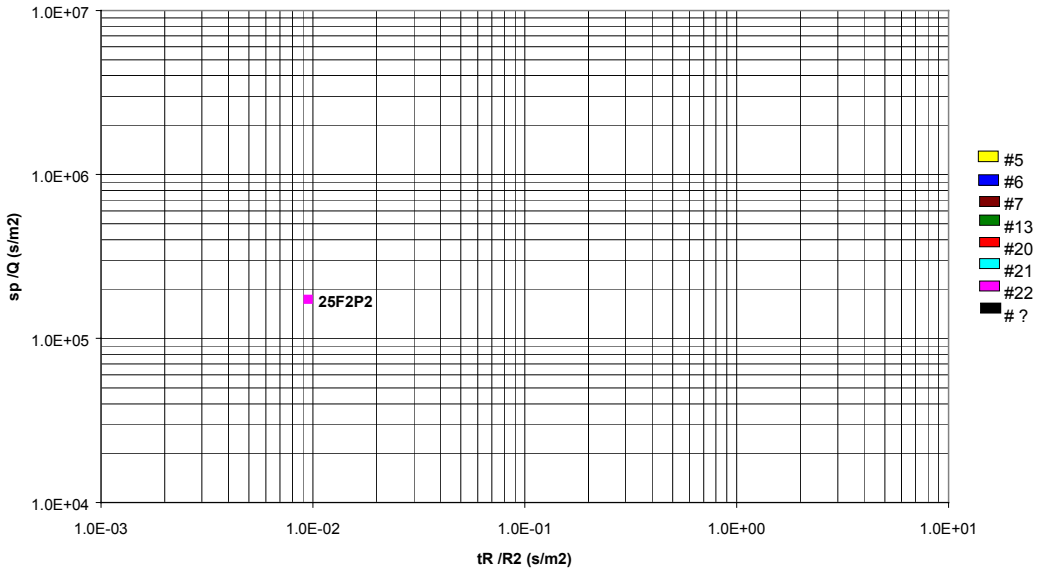

APPENDIX 4: Drawdown-time/distance^{2}plots from the short-term interference tests inKI0025F03.

GEOSIGMA AB P.O. Box 894 S-751 08 Uppsala Sweden	Pumping test analysis Theis analysis method Confined aquifer	Page 1 Project: TRUE BLOCK SCALE Evaluated by: JEL | Date: 1999-12-17

Pumping Test No. Test #2a. Sink:KI0025F03:52-54 m	Test conducted on: 1999-10-05
Drawdown vs. t/R2 (Primary responses)	

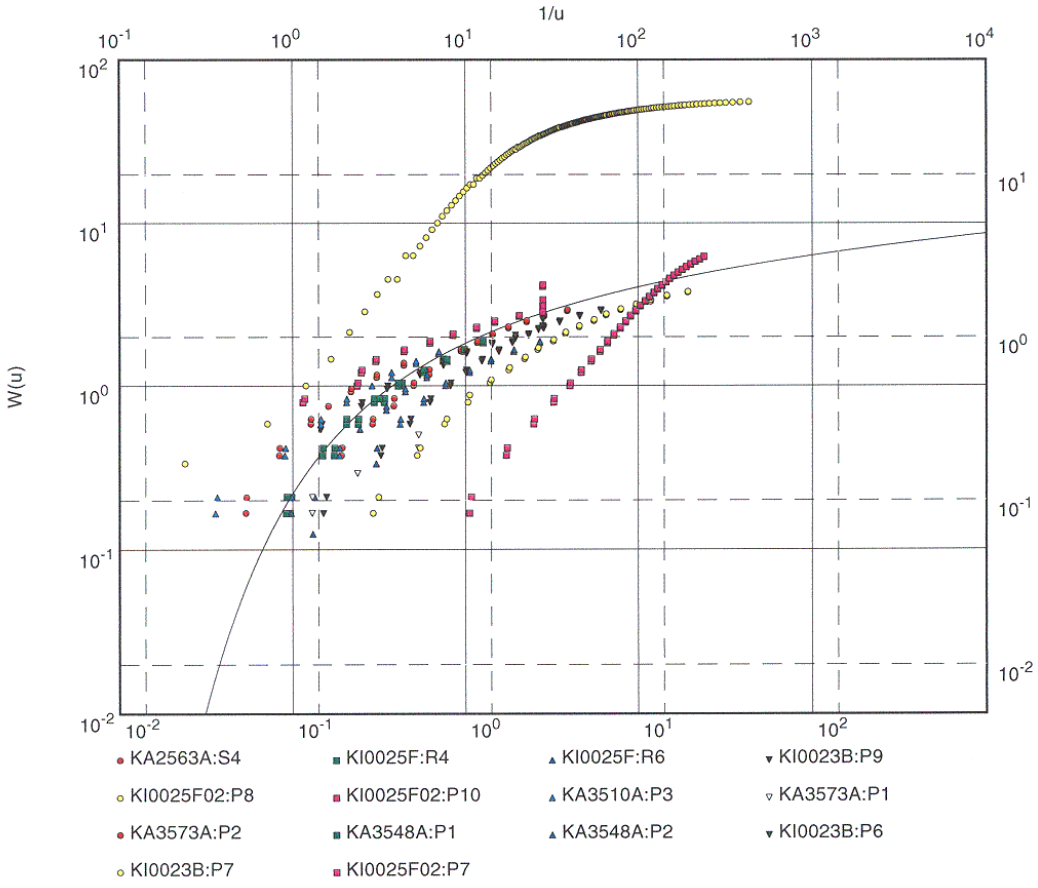

For Theis' type curve shown in the diagram:

T=2.36E-6 m2/s S=6.69E-7 tp=34 mins

Data curves: X-axis: time/distance squared (s/m2)
Y-axis: Drawdown (m)

GEOSIGMA AB P.O. Box 894 S-751 08 Uppsala Sweden	Pumping test analysis Theis analysis method Confined aquifer	Page 2 Project: TRUE BLOCK SCALE Evaluated by: JEL | Date: 1999-12-17

Pumping Test No. Test #2b. Sink:KI0025F03:51.5-53.5 m	Test conducted on: 1999-10-06
Drawdown vs. t/R2 (Primary responses)	

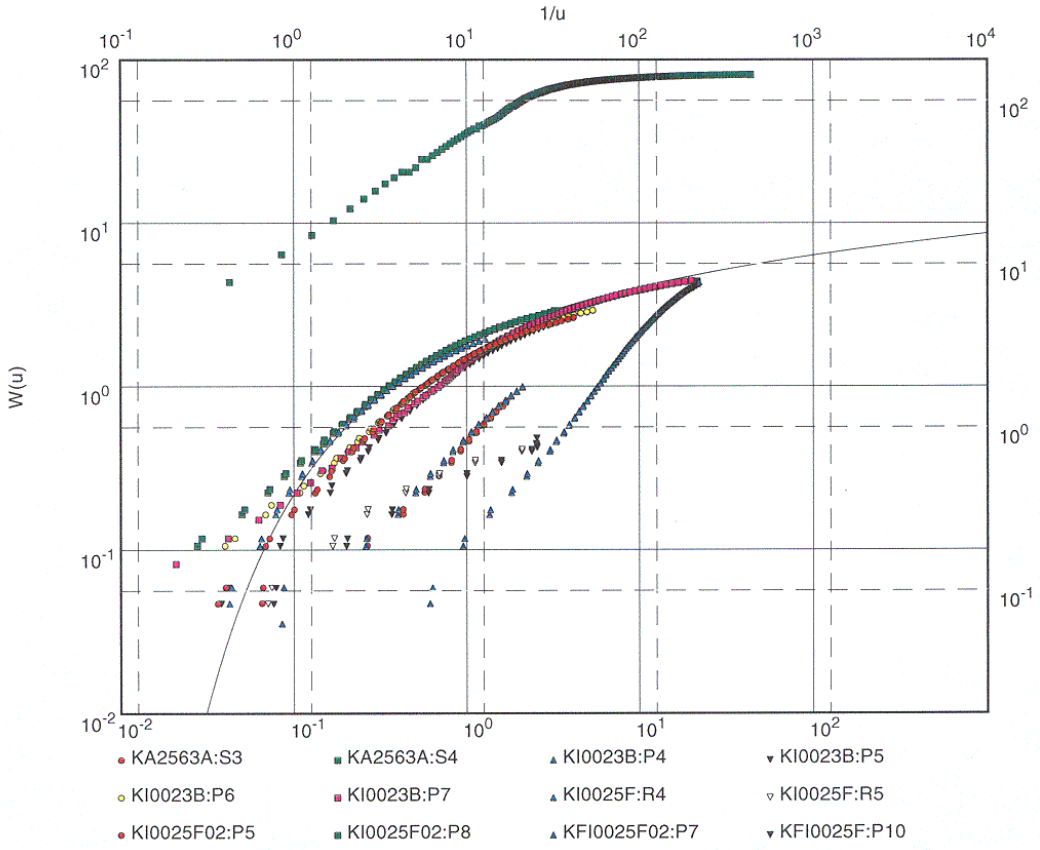

For Theis' type curve match shown in diagarm:

T=1.70E-6 m2/s
S=5.40E-7

GEOSIGMA AB P.O. Box 894 S-751 08 Uppsala Sweden	Pumping test analysis Theis analysis method Confined aquifer	Page 3 Project: TRUE BLOCK SCALE Evaluated by: JEL | Date: 1999-12-17

Pumping Test No. Test #7. Sink:KI0025F03:72-74 m	Test conducted on: 1999-10-07
Drawdown vs. t/R2 (All responses)	

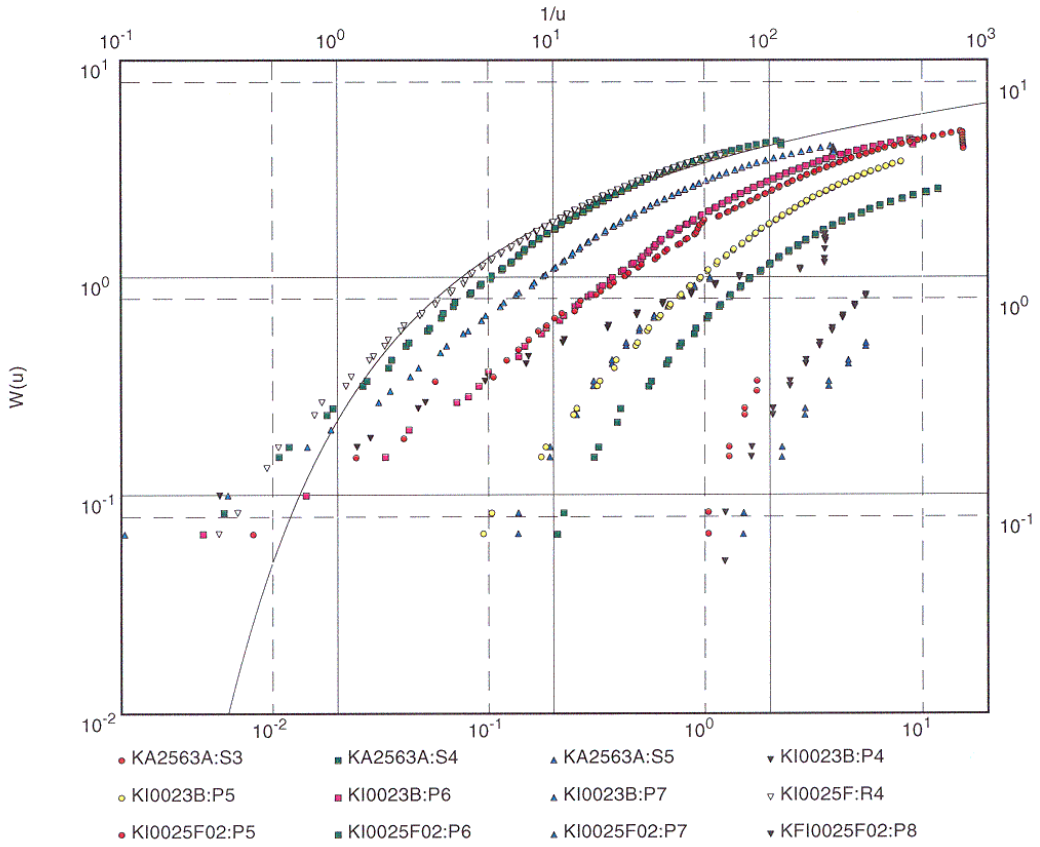

For type curve match in diagram:

T=9.35E-7 m2/s
S=7.46E-8

GEOSIGMA AB P.O. Box 894 S-751 08 Uppsala Sweden	Pumping test analysis Theis analysis method Confined aquifer	Page 4 Project: TRUE BLOCK SCALE Evaluated by: JEL | Date: 1999-12-17

Pumping Test No. Test #9. Sink:KI0025F03:87-89 m	Test conducted on: 1999-10-08
Drawdown vs. t/R2 (Primary responses)	

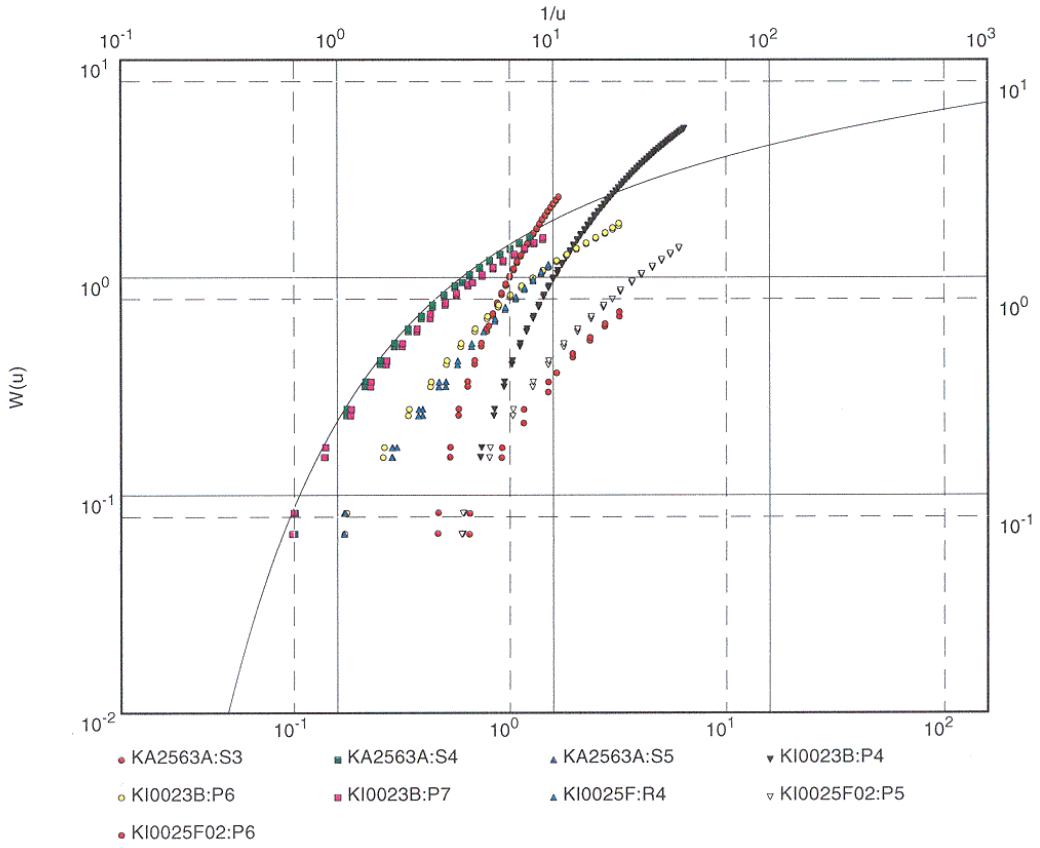

For Theis' type curve match in diagram:

T=8.34E-7 m2/s
S=5.28E-7

APPENDIX 5: Straight-line distances between sink and receiver sections for the short-term interference tests in KI0025F03.

Borehole	Test #1	Test #2a	Test #2b	Test #3	Test #4	Test #5	Test #6	Test #7	Test #8	Test #9	Test #10	Test #11	Test #12
KA2563A:S1		72	72					57		50			49
KA2563A:S2		66	66					52		45			49
KA2563A:S3		39	39					31		33			59
KA2563A:S4		27	27					29		38			70
KA2563A:S5		26	26					41		54			89
KI0025F:R1	143	136	136					118		106			
KI0025F:R2	129	121	121					102		91			
KI0025F:R3	89	82	82					66		64			
KI0025F:R4	52	45	45					40		34			
KI0025F:R5	30	26	26					28		37			
KI0025F:R6	24	32	32					53		67			
KI0023B:P1	118	109	109					89		76			44
KI0023B:P2	68	60	60					41		29			27
KI0023B:P3	55	47	47					29		20			35
KI0023B:P4	42	34	34					18.5		17			46
KI0023B:P5	35	27	27					15		19			52
KI0023B:P6	28	21	21					14.5		24			59
KI0023B:P7	15	11	11					22		36			72
KI0023B:P8	9	15	15					35		49			86
KI0023B:P9	23	32	32					53		68			105
KI0025F02:P1	128	119	119	116	114	110	108	99	86	85	81	74	50
KI0025F02:P2	91	82	82	79	77	73	71	62	50	48	45	38	21
KI0025F02:P3	54	45	45	42	41	37	35	26	17	16	14	14	33
KI0025F02:P4	43	35	35	32	30	26	25	17	13	13	14	19	43
KI0025F02:P5	33	25	25	22	21	17	16	11	16	17	20	27	52
KI0025F02:P6	25	18	18	15	14	11	10	12	22	23	27	34	59
KI0025F02:P7	18	11	11	9	9	9	10	17	29	30	34	41	67
KI0025F02:P8	12	8	8	8	9	12	14	23	35	37	41	48	74
KI0025F02:P9	7	14	14	16	18	22	24	34	47	48	52	60	85
KI0025F02:P10	23	32	32	35	37	41	43	53	66	68	72	79	105
KA3510A:P1		111	111										
KA3510A:P2		91	91										
KA3510A:P3		60	60										
KA3573A:P1		66	66										
KA3573A:P2		80	80										
KA3548A:P1		57	57										
KA3548A:P2		65	65										